

Azimuthal Jet Flavor Tomography via CUJET with Running Coupling in 2+1D Viscous QGP Fluids

Jiechen Xu

with Miklos Gyulassy & Alessandro Buzzatti

For New Frontiers in QCD 2013, YITP, Kyoto, Japan



Outline

❖ Overview

- Jet Tomography
- DGLV opacity expansion
- Dynamical medium effect
- Elastic energy loss

❖ CUJET1.0

- Fixed Coupling DGLV (fcDGLV) + Elastic + Bjorken
- Results of light and heavy flavors

❖ Running Coupling

- In radiative and elastic energy loss
- Results of running coupling CUJET1.0

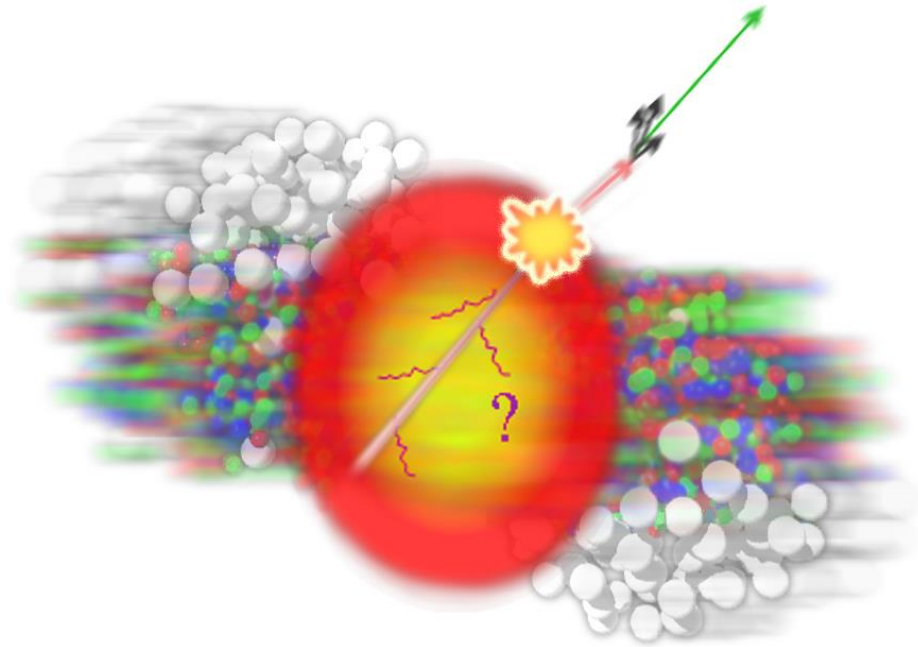
❖ CUJET2.0

- Running Coupling DGLV (rcDGLV) + Elastic + VISH2+1
- Results
 - ❑ Light and heavy flavor R_{AA} at RHIC and LHC
 - ❑ Jet transport coefficient \hat{q}
 - ❑ Single particle anisotropy v_2

❖ Summary and Outlook

Jet Tomography

- ❖ Hard processes happen before the formation of the medium
 - Hard parton production in AA collisions can be calculated in the pQCD paradigm
- ❖ Quarks and gluons have final state interaction
 - Parton shower will be modified by interacting with the medium
- ❖ One can use quark or glue jet as a probe, and measure the quenching pattern of hadron/lepton jet fragments, and gain information about the QGP evolution profile
 - Or the other way: with a known medium density evolution to study the parton medium interaction mechanism



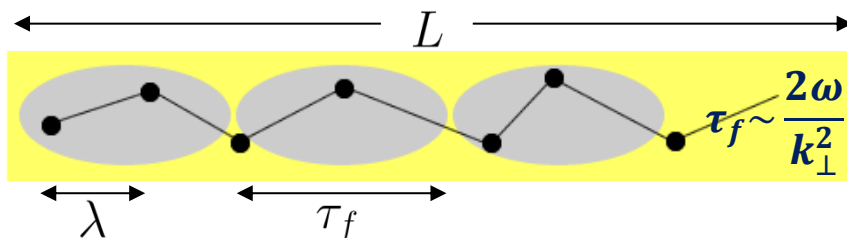
Radiative Energy Loss

❖ Jet quenching models have been formulated in the pQCD framework based on different underlying assumptions about the parton-medium interaction

- Finite temperature field theory (AMY)
- Higher twist (HT)
- Multiple soft scattering (BDMPS-Z and ASW)
- Opacity expansion (GLV)

❖ GLV

- The plasma is modeled by a series of static or dynamical scattering centers.
- Energy loss is formulated as an expansion in the number of parton-medium scatterings (opacity expansion)
 - ❑ Dominated by the first hard contribution. (“Thin plasma”)
- Include the power-law tail of the scattering cross section.



- ❑ $\tau_f < \lambda < L$ Incoherent multiple collisions
- ❑ $\lambda < \tau_f < L$ LPM effect
- ❑ $\lambda < L < \tau_f$ Factorization limit

DGLV Opacity Expansion (Gyulassy, Levai, Vitev, Djordjevic)

$$x \frac{dN^{(n)}}{dx d^2\mathbf{k}} = \frac{C_R \alpha_s}{\pi^2} \frac{1}{n!} \int \prod_{i=1}^n \left(d^2\mathbf{q}_i \frac{L}{\lambda_g(i)} \left[\bar{v}_i^2(\mathbf{q}_i) - \delta^2(\mathbf{q}_i) \right] \right) \times$$

$$\times \left(-2 \tilde{\mathbf{C}}_{(1,\dots,n)} \cdot \sum_{m=1}^n \tilde{\mathbf{B}}_{(m+1,\dots,n)(m,\dots,n)} \left[\cos \left(\sum_{k=2}^m \Omega_{(k,\dots,n)} \Delta z_k \right) - \cos \left(\sum_{k=1}^m \Omega_{(k,\dots,n)} \Delta z_k \right) \right] \right)$$

Opacity series expansion $\rightarrow \left(\frac{L}{\lambda}\right)^n$

Soft Radiation ($E \gg \omega, x \ll 1$)
Soft Scattering ($E \gg q, \omega \gg k_T$)

Radiation antenna \rightarrow Cascade terms

$$\tilde{\mathbf{C}}_{(i_1 i_2 \dots i_m)} = \frac{(\mathbf{k} - \mathbf{q}_{i_1} - \mathbf{q}_{i_2} - \dots - \mathbf{q}_{i_m})}{(\mathbf{k} - \mathbf{q}_{i_1} - \mathbf{q}_{i_2} - \dots - \mathbf{q}_{i_m})^2 + m_g^2 + M^2 x^2},$$

$$\tilde{\mathbf{B}}_{(i_1 i_2 \dots i_m)(j_1 j_2 \dots j_n)} = \tilde{\mathbf{C}}_{(i_1 i_2 \dots j_m)} - \tilde{\mathbf{C}}_{(j_1 j_2 \dots j_n)}.$$

Gunion-Bertsch

$$\tilde{\mathbf{B}}_i = \tilde{\mathbf{H}} - \tilde{\mathbf{C}}_i,$$

Hard

$$\tilde{\mathbf{H}} = \frac{\mathbf{k}}{\mathbf{k}^2 + m_g^2 + M^2 x^2},$$

LPM effect \rightarrow

$$\Omega_{(m,\dots,n)} = \underbrace{\frac{(\mathbf{k} - \mathbf{q}_m - \dots - \mathbf{q}_n)^2}{2xE}}_{\text{Inverse formation time}} + \underbrace{\frac{m_g^2 + M^2 x^2}{2xE}}_{\text{Mass effects}}$$

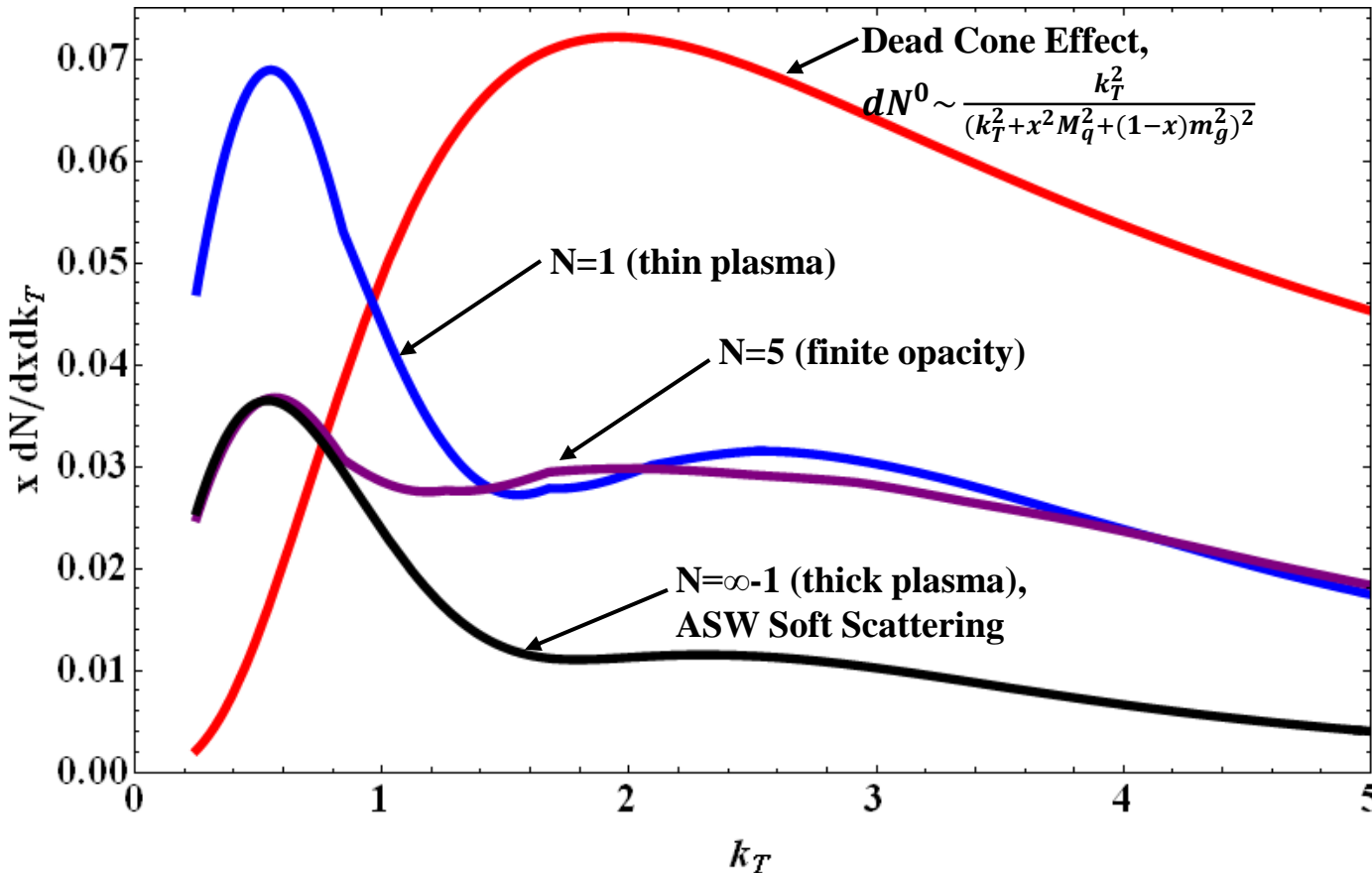
Inverse formation time Mass effects

Scattering center distribution $\rightarrow \Delta z_k = z_k - z_{k-1} \sim L/(n+1)$

Debye and thermal gluon mass $\rightarrow \mu = gT \sqrt{1 + N_f/6}, m_g = \mu/\sqrt{2}$ (HTL)

Higher order opacity: k_T distribution

$E=20\text{GeV}$, $x=0.25$, bottom quark, $\alpha=0.3$, $T=250\text{MeV}$, $L=5\text{fm}$, $\lambda=1\text{fm}$, $\mu=0.5\text{GeV}$, Opacity Order = N



Buzzatti,
Ficnar,
Gyulassy,
unpublished

- Area below the curve is the radiative energy loss for a given initial energy and energy fraction.
- Comparing to 5th order in opacity, 1st order result has only 20% energy loss difference → higher order correlations make opacity series less separated in scale
- At low k_T , opacity series quickly converge to the multi soft scattering limit
- At high k_T , opacity series show rather stable Landau tail → In incoherent and LPM regime, first order dominates
- ASW has no Landau tail → 1st order is not included in the theory
- Open question: running coupling effect on different opacities

Effective Potential

Static potential (DGLV)

$$|\bar{v}_i(q_i)|^2 = \frac{1}{\pi} \frac{\mu(z_i)^2}{(q^2 + \mu(z_i)^2)^2}$$

- ❖ Static scattering centers
- ❖ Color-electric screened Yukawa potential (Debye mass)
- ❖ Full opacity series

Dynamical potential [Djordjevic and Heinz; Gelis; Zakharov]

$$|\bar{v}_i(q_i)|^2 = \frac{1}{\pi} \frac{\mu(z_i)^2}{q^2 (q^2 + \mu(z_i)^2)}$$

- ❖ Scattering centers recoil
- ❖ Includes not screened color-magnetic effects (HTL gluon propagators)
- ❖ Only first order in opacity

Interpolating potential (CUJET)

$$|\bar{v}_i(q_i)|^2 = \frac{\mathcal{N}(\mu_e, \mu_m)}{\pi} \frac{\mu_e(z_i)^2}{(q^2 + \mu_e(z_i)^2)(q^2 + \mu_m(z_i)^2)}$$

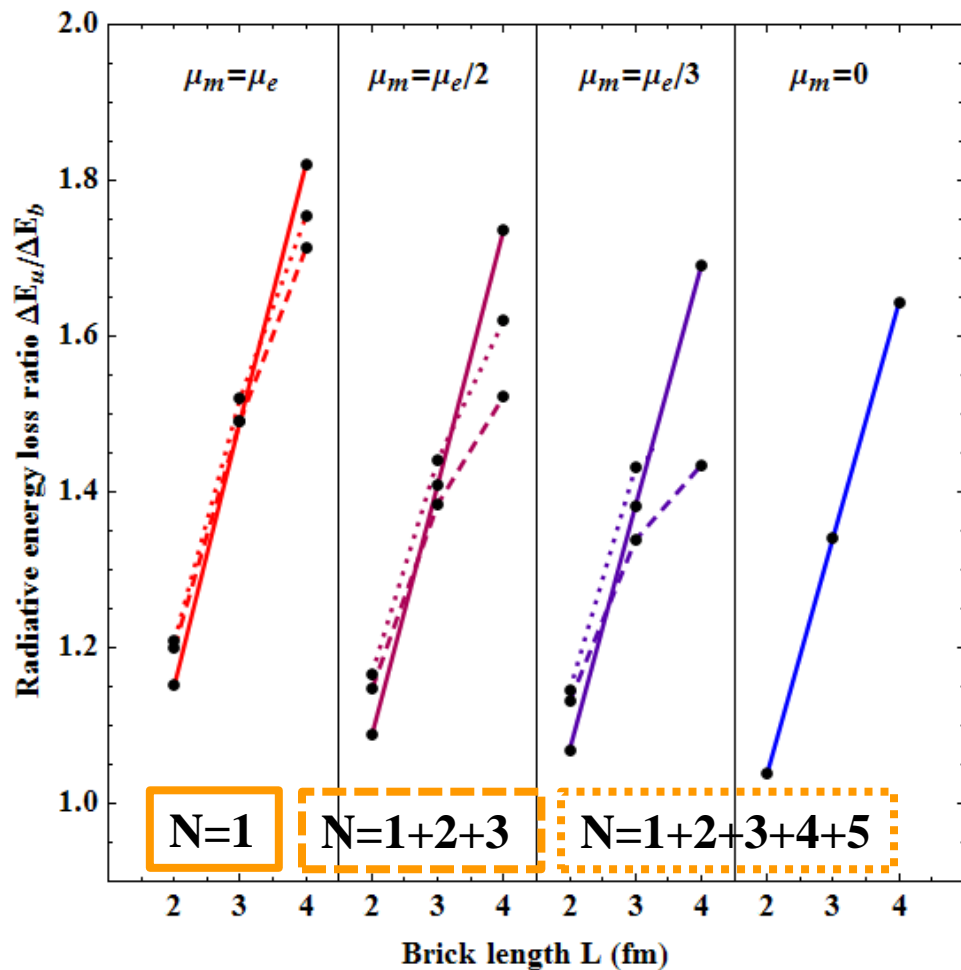
$\mu_e = f_E \mu$
 $\mu_m = f_M \mu$

- Introduces effective color-magnetic mass
- Add f_E and f_M allows one to interpolate between the static and dynamical limits, and further explore Non-HTL regime
- Magnetic screening allows full opacity series

Dynamical potential effect

- ❖ Interpolate between Static and Dynamical potential with a new effective potential

$$\frac{1}{(q^2 + \mu^2)^2} \xleftarrow{\text{Static}} \frac{1}{(q^2 + \mu_m^2)(q^2 + \mu_e^2)} \xrightarrow{\text{Dynamical}} \frac{1}{q^2(q^2 + \mu^2)}$$



Buzzatti and Gyulassy, NPA (2011)

- ❖ Uniform static brick; $E=20\text{GeV}$, $T=250\text{MeV}$, $\lambda=1\text{fm}$, $\mu=0.5\text{GeV}$, $\alpha=0.3$, Opacity Order = N
- ❖ $\left(\frac{\Delta E_u}{\Delta E_b}\right)$ ratio decreases when increasing color magnetic screening length
- ❖ Long range dynamical color magnetic screening in the HTL framework may significantly enhance the bottom quark radiative energy loss and thereby help solve the heavy quark puzzle
- ❖ Open question: running coupling effect on heavy quark energy loss

Elastic energy loss and Fluctuations

❖ Bjorken elastic collisions: $\frac{dE}{dx} = -\pi C_R \frac{\alpha^2}{\beta^2} \left(1 + \frac{n_f}{6}\right) \log B, B = \frac{E}{Q^*}$

❖ Thoma-Gyulassy model [Thoma & Gyulassy, NPB (1991)], employed the use of HTL gluon propagators to provide a more natural infrared regulator

$$\frac{dE}{dx} = \frac{4\pi}{3} C_F \alpha_s^2 T^2 \left(\frac{1}{v} + \frac{v^2 - 1}{2v^2} \log \frac{1+v}{1-v} \right) \log \left(\frac{k_{max}}{\mu_D} \right)$$

➤ Very similar to Bjorken computation, with only a different Coulomb log reflecting more natural cutoffs. Elastic EL treatment can also be found in [Barteen & Thoma, PRD (1991)]

❖ Energy loss fluctuations: The probability of losing a fractional energy $\epsilon = \frac{\Delta E}{E}$ is the convolution of Radiative and Elastic contributions

$$P(\epsilon) = \int dx P_{rad}(\epsilon) P_{el}(x - \epsilon)$$

ASSUME Poisson distribution for the number of INCOHERENTLY emitted gluons

➤ **Radiative:** $P_{rad}(\epsilon) = P_0 \delta(\epsilon) + \tilde{P}(\epsilon)|_0^{\epsilon_{MAX}} + P_1 \delta(\epsilon_{MAX} - \epsilon)$

➤ **Elastic:** $P_{el}(\epsilon) = e^{-\bar{N}_c} \delta(\epsilon) + \mathcal{N} e^{-\frac{(\epsilon - \bar{\epsilon})^2}{4T\bar{\epsilon}/E}}$

Gaussian fluctuation for multiple collisions

CUJET1.0

❖ Geometry

- Glauber model
- Bjorken longitudinal expansion

❖ Energy loss

- DGLV – MD Radiative energy loss model
- TG Elastic energy loss model
- Path length fluctuations, Energy loss fluctuations
- Full dynamical computation:

$$x \frac{dN_g^{DYN}}{dx} = \frac{18C_{R\alpha_s^3}}{\pi^2} c_d(n_f) \int dz \rho(z) \int d^2\mathbf{q} \int d^2\mathbf{k} \frac{1}{q^2(q^2 + \mu^2(z))} \\ \times \frac{2(\mathbf{k} - \mathbf{q})}{(\mathbf{k} - \mathbf{q})^2 + \chi^2} \left(\frac{(\mathbf{k} - \mathbf{q})}{(\mathbf{k} - \mathbf{q})^2 + \chi^2(z)} - \frac{\mathbf{k}}{\mathbf{k}^2 + \chi^2(z)} \right) \\ \times \left(1 - \cos \left(\frac{(\mathbf{k} - \mathbf{q})^2 + \chi^2(z)}{2Ex} z \right) \right),$$

$$\vec{z} = \vec{x}_0 + \hat{\Omega}\tau, z = |\vec{z}|$$

$$\mu(\vec{z}) = g(T(\vec{z}))T(\vec{z})\sqrt{1 + N_f/6}$$

$$m_g(\vec{z}) = \mu(\vec{z})/\sqrt{2}$$

$$\chi(\vec{z}) = M^2 x^2 + m_g^2(\vec{z})(1 - x)$$

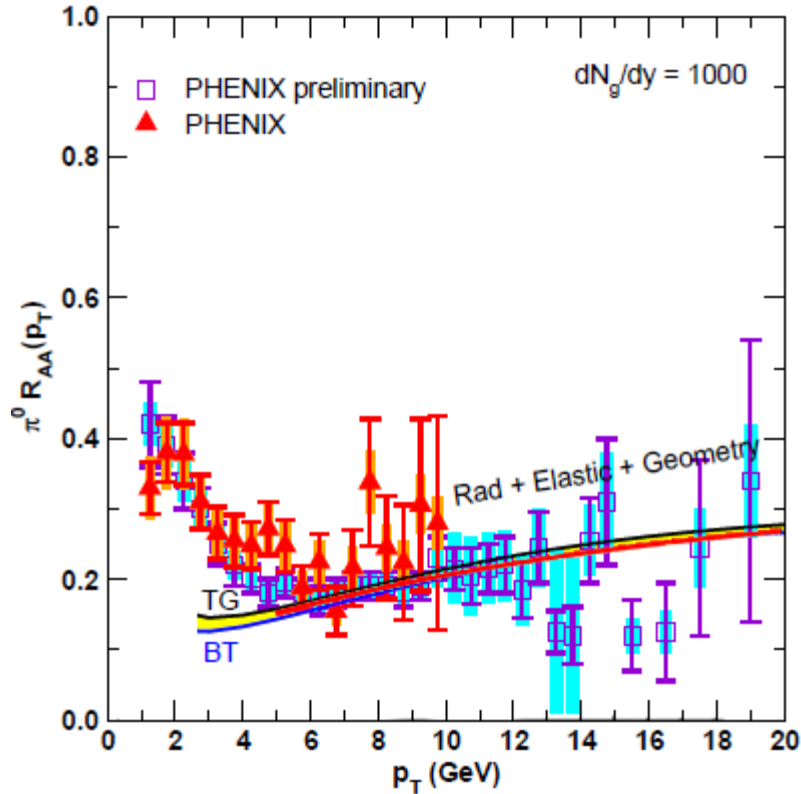
❖ Detailed convolution over initial production spectra (LO pQCD CTEQ5, NLO/FONLL)

❖ In vacuum Fragmentation Functions (KKP, Peterson, VOGT)

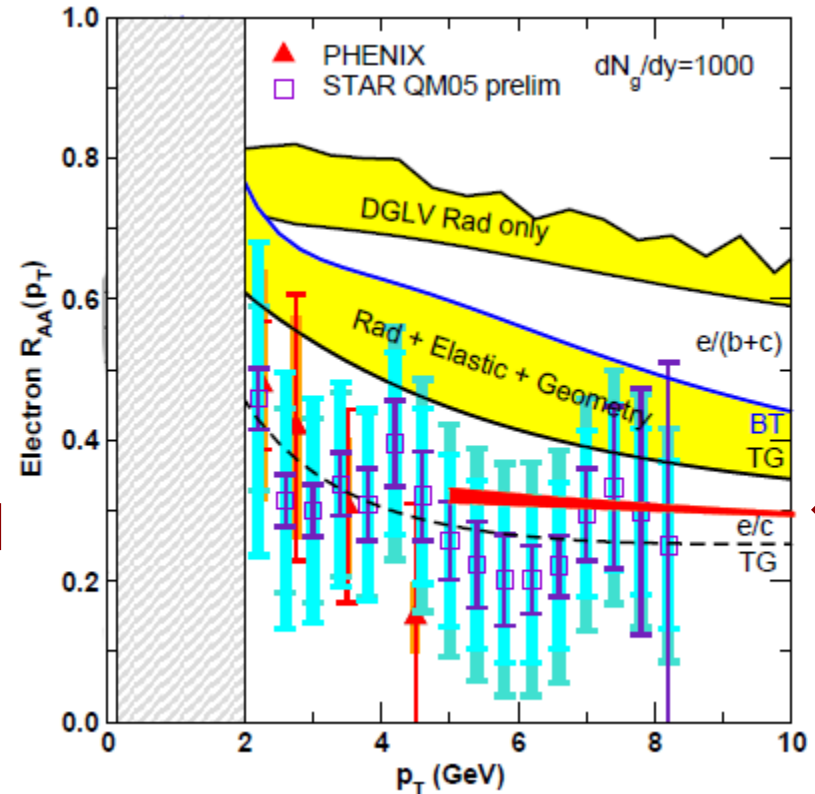
Possibility to evaluate systematic theoretical uncertainties such as sensitivity to formation and decoupling phases of the QGP evolution, local running coupling and screening scale variations, and other effects out of reach with analytic approximations

CUJET1.0: Pions and Electrons at RHIC

LIGHT QUARKS



HEAVY QUARKS

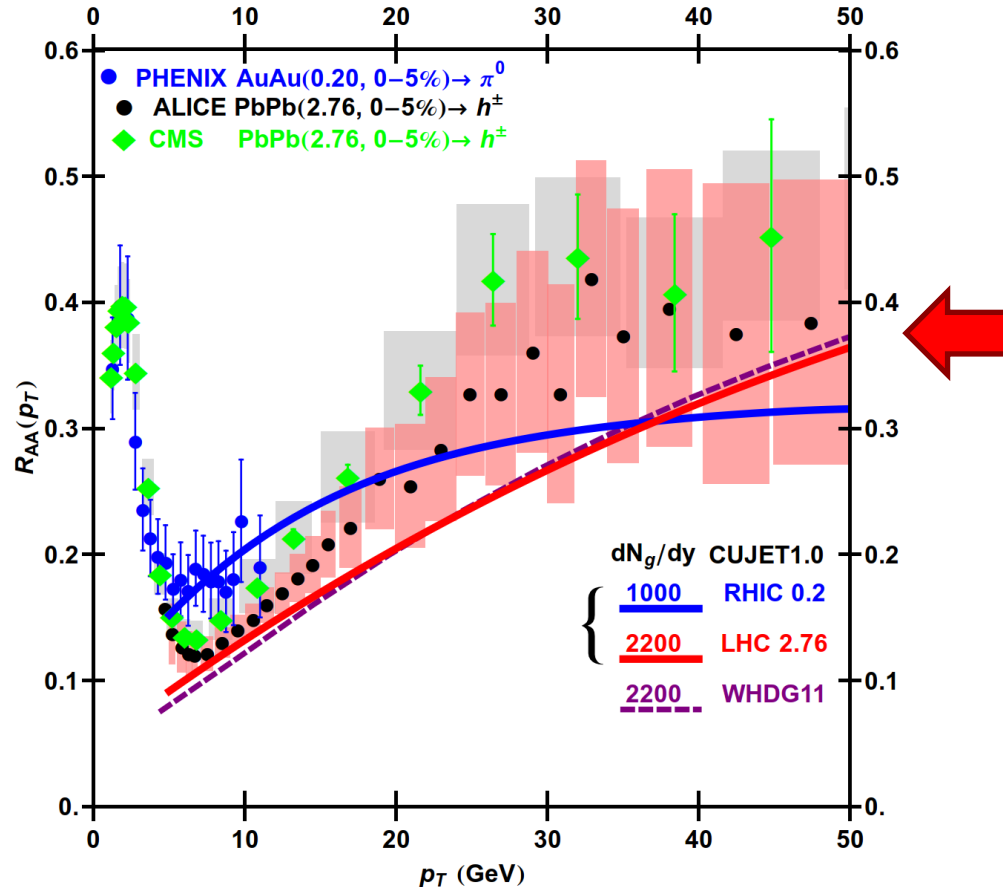


Wicks, Horowitz, Djordjevic, Gyulassy / NPA (2007)

- ❖ Taking into account elastic energy loss and dynamical scattering effect, CUJET1.0 is able to explain non-photonic electron R_{AA} at RHIC while being compatible with pion data

CUJET1.0: Pions at LHC

A. Buzzatti and M. Gyulassy, PRL 108, 0223101 (2012); See also B. Betz and M. Gyulassy, arXiv:1201.02181



- ❖ Pion R_{AA} from Fixed Coupling CUJET at LHC is overquenched \rightarrow cannot explain the surprising transparency
- ❖ Extended energy range probed at LHC \rightarrow Running Coupling

Running Coupling DGLV model

$$\alpha\left(\frac{k_{\perp}^2}{x(1-x)}\right) \alpha(q^2)^2$$

$$x \frac{dN^{(n)}}{dx d^2\mathbf{k}} = \frac{C_R \alpha_s}{\pi^2} \frac{1}{n!} \int \prod_{i=1}^n \left(d^2\mathbf{q}_i \frac{L}{\lambda_g(i)} [v_i^2(\mathbf{q}_i) - \delta^2(\mathbf{q}_i)] \right) \times$$

$$\times \left(-2 \tilde{\mathbf{C}}_{(1,\dots,n)} \cdot \sum_{m=1}^n \tilde{\mathbf{B}}_{(m+1,\dots,n)(m,\dots,n)} \left[\cos \left(\sum_{k=2}^m \Omega_{(k,\dots,n)} \Delta z_k \right) - \cos \left(\sum_{k=1}^m \Omega_{(k,\dots,n)} \Delta z_k \right) \right] \right)$$

Opacity series expansion $\rightarrow \left(\frac{L}{\lambda}\right)^n$

Soft Radiation ($E \gg \omega, x \ll 1$)
Soft Scattering ($E \gg q, \omega \gg k_T$)

Radiation antenna \rightarrow Cascade terms

$$\tilde{\mathbf{C}}_{(i_1 i_2 \dots i_m)} = \frac{(k - \mathbf{q}_{i_1} - \mathbf{q}_{i_2} - \dots - \mathbf{q}_{i_m})}{(k - \mathbf{q}_{i_1} - \mathbf{q}_{i_2} - \dots - \mathbf{q}_{i_m})^2 + m_g^2 + M^2 x^2},$$

$$\tilde{\mathbf{B}}_{(i_1 i_2 \dots i_m)(j_1 j_2 \dots j_n)} = \tilde{\mathbf{C}}_{(i_1 i_2 \dots j_m)} - \tilde{\mathbf{C}}_{(j_1 j_2 \dots j_n)}$$

Gunion-Bertsch

$$\tilde{\mathbf{B}}_i = \tilde{\mathbf{H}} - \tilde{\mathbf{C}}_i,$$

Hard

$$\tilde{\mathbf{H}} = \frac{\mathbf{k}}{k^2 + m_g^2 + M^2 x^2},$$

$$\alpha(4T^2)$$

LPM effect \rightarrow

$$\Omega_{(m,\dots,n)} = \underbrace{\frac{(k - \mathbf{q}_m - \dots - \mathbf{q}_n)^2}{2xE}}_{\text{Inverse formation time}} + \underbrace{\frac{m_g^2 + M^2 x^2}{2xE}}_{\text{Mass effects}}$$

Inverse formation time Mass effects

Scattering center distribution \rightarrow

$$\Delta z_k = z_k - z_{k-1} \sim L/(n+1)$$

Debye and thermal gluon mass \rightarrow

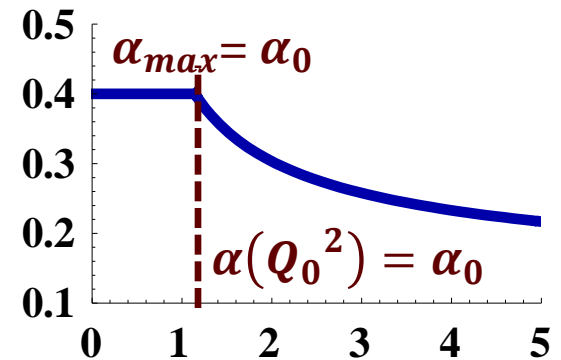
$$\mu = gT \sqrt{1 + N_f/6}, m_g = \mu/\sqrt{2} \text{ (HTL)}$$

Multi-scale Running Coupling: Radiative

❖ Introduce one-loop alpha running

$$\alpha_s \longrightarrow \alpha_s(Q^2) = \begin{cases} \alpha_0 & \text{if } Q \leq Q_0 \\ \frac{2\pi}{9 \log(Q/\Lambda_{QCD})} & \text{if } Q > Q_0 \end{cases}$$

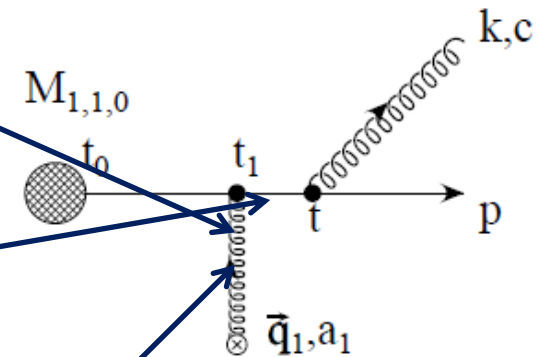
B. G. Zakharov, JETP Lett. 88 (2008) 781-786



➤ Two powers $\alpha(Q^2)$ originate from the jet-medium interaction vertices; the exchanged momentum is q , and $Q^2 = q^2$

➤ One power $\alpha(Q^2)$ originates from the radiated gluon vertex; the exchanged momentum is the Mandelstam variable \hat{t} and

$$Q^2 = \hat{t}^2 \approx \frac{k_{\perp}^2}{x(1-x)} + \frac{M_q^2}{1-x} + \frac{m_g^2}{x}$$



➤ One power of the thermal coupling originates from the Debye mass $m_D(\alpha(Q^2), T)$; the scale is set to be proportional to the temperature of the plasma, $Q^2 = (2T)^2$

Multi-scale Running Coupling: Elastic

- ❖ S. Peigne and A. Peshier, PRD 77, 114017 (2008)
- ❖ In the limit of $E \gg k$ (the momentum of target particle in the medium), approximate parton-parton elastic cross section as $\frac{d\sigma_{i,j}}{d\hat{t}} = \frac{2\pi\alpha^2}{\hat{t}^2} c_{i,j}$
- ❖ Energy loss per unit length

$$\frac{dE}{dx} = \int d^3k \rho_i(k) \Phi \int_{\hat{t}_{MIN}}^{\hat{t}_{MAX}} d\hat{t} \frac{d\sigma_{i,j}}{d\hat{t}} \cdot (E - E')$$

$$E - E' = -\frac{\hat{t}}{2k(1 - \cos\theta)}$$

$$\Phi = 1 - \cos\theta .$$

$$\frac{dE}{dx} = -\pi C_R \frac{\alpha^2}{\beta^2} \left(1 + \frac{n_f}{6}\right) \log B \longleftrightarrow \frac{dE}{dx} = \frac{4\pi}{3} C_F \alpha_s^2 T^2 \left(\frac{1}{v} + \frac{v^2 - 1}{2v^2} \log \frac{1+v}{1-v}\right) \log\left(\frac{k_{max}}{\mu_D}\right)$$

$$\alpha_s^2 \int_{\mu^2}^{4ET} \frac{d\hat{t}}{\hat{t}} \longrightarrow \int_{\mu^2}^{4ET} \frac{d\hat{t}}{\hat{t}} \alpha_s^2(\hat{t}) \quad q_{\perp}^{MAX} = \sqrt{4ET}$$

$$\alpha_s(|t|) = [4\pi\beta_0 \ln(|t|/\Lambda^2)]^{-1}$$

$$\alpha_s^2 \log \frac{4ET}{\mu^2} \longrightarrow \alpha_s(\mu^2) \alpha_s(4ET) \log \frac{4ET}{\mu^2 (\alpha_s(4T^2); T)}$$

a-b-c model and running coupling

A. Buzzatti, Thesis

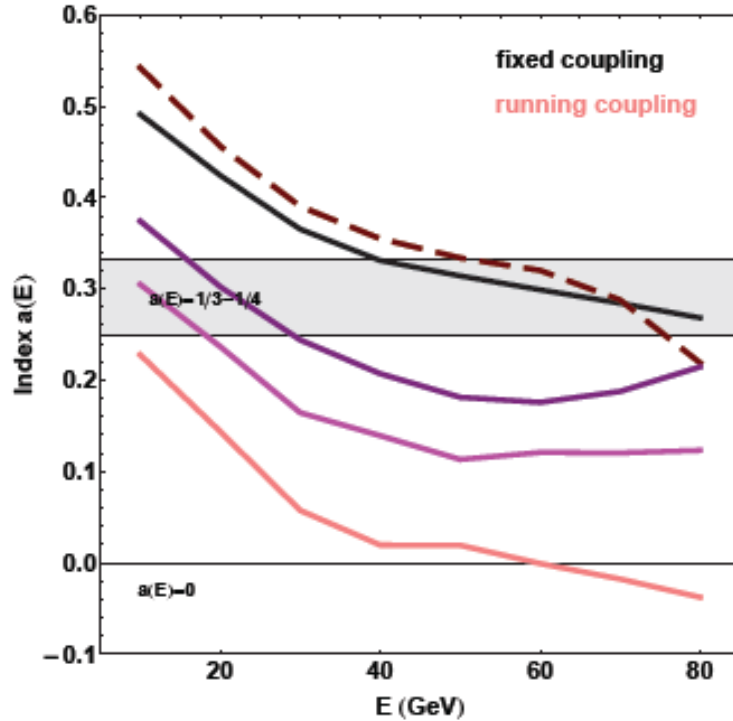


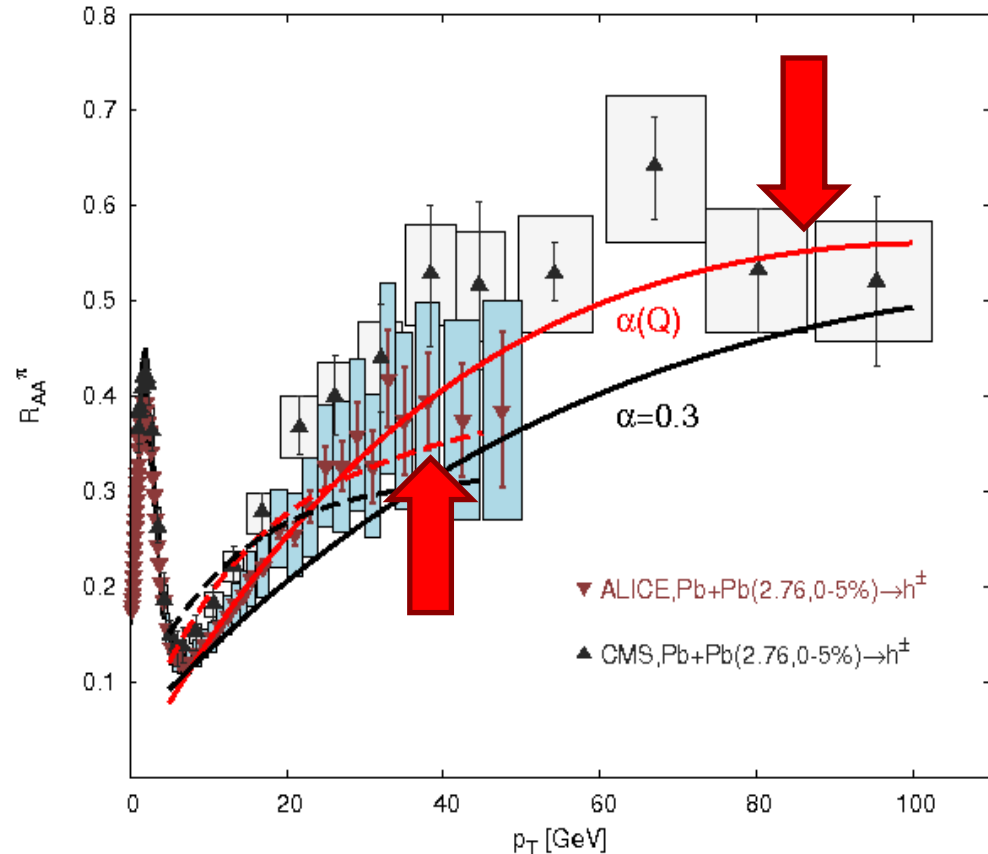
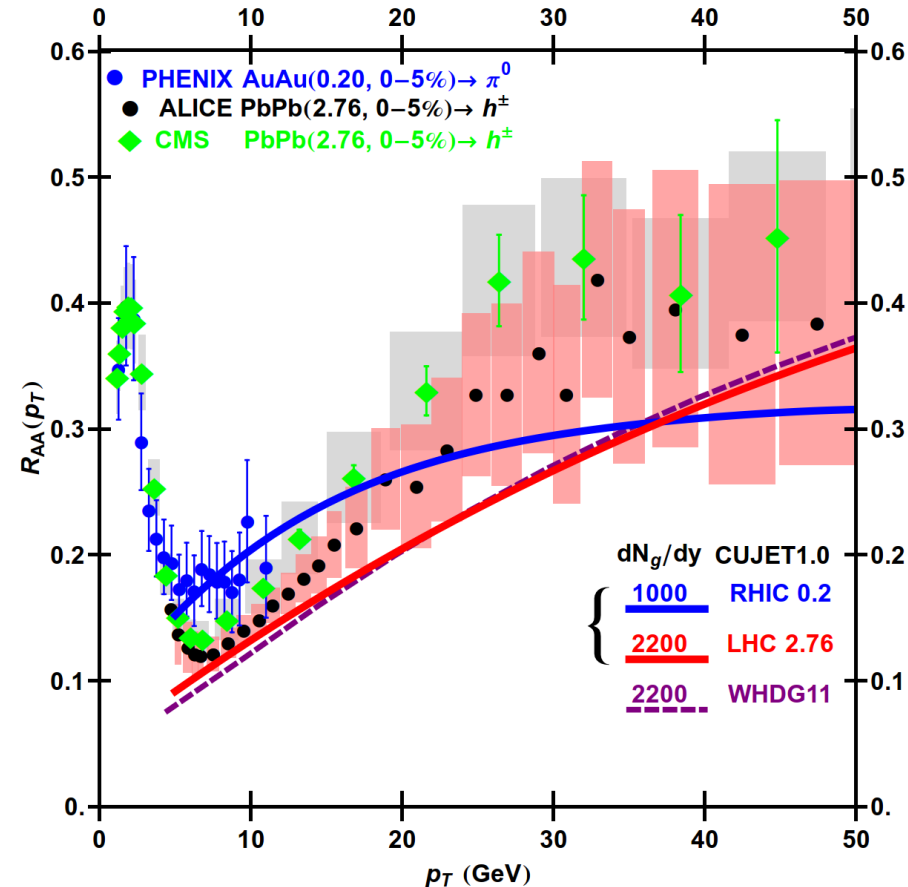
Figure 4.9: Index $a(E)$ (cf. Eq. (4.29)) for different assumptions of the running coupling: fixed effective $\alpha_s = 0.3$ (black), only thermal coupling running (dashed red), only $\alpha_s^2(q_\perp^2)$ running (purple), only $\alpha_s^2(k_\perp^2/(x(1-x)))$ running (magenta), all couplings running (pink). The saturated α_0 value is chosen equal to 0.4, which corresponds to approximately $Q_0 \sim 1$ GeV. The plot shows the energy loss of a light quark traveling through a gluonic plasma of size 5 fm. The density profile resembles the medium created in a Pb-Pb head-on collision.

- ❖ $\frac{dP}{d\tau} = -\kappa P^a \tau^b T^{2-a+b}$
- ❖ Asymptotic LPM behavior of GLV model

$$\frac{\Delta E}{E} \propto T^3 L^2 \frac{\log(E/T)}{E}$$
 - Fixed coupling: $a \sim 1/3 - 1/4$
- ❖ Thermal coupling has less effect since T needs to be > 0.6 GeV to run for $Q_0 \sim 1$ GeV
- ❖ Comparing to $\alpha(k_\perp^2/(x(1-x)))$, $\alpha(q_\perp^2)$ contributes less since q_\perp peaks at small values of q_\perp , while k_\perp has a Landau tail
 - ❖ Full running shows no $\Delta E/E$ dependence on E , therefore $a \sim 0$
 - ➔ Integration from scattering cross section has $1/\log E$ to cancel the LPM $\log E$ dependence
 - ➔ $1/\log E$ falls steeper than power law, lead to smearing of the Landau tail in k_\perp distribution

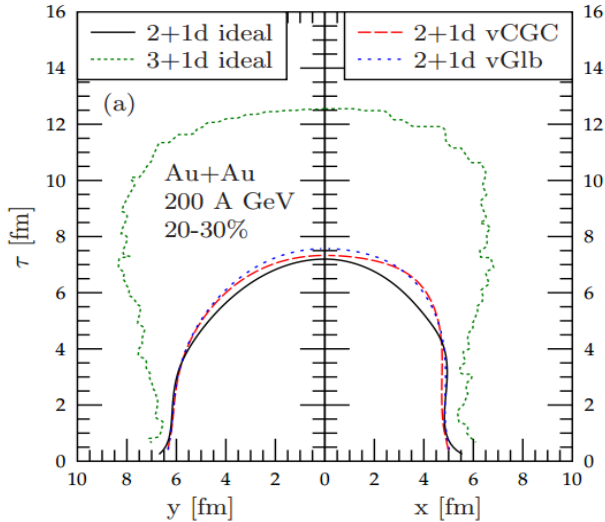
CUJET1.0: Pions at LHC

A. Buzzatti and M. Gyulassy, PRL 108, 0223101 (2012); See also B. Betz and M. Gyulassy, arXiv:1201.02181



Running Coupling CUJET1.0 explains the surprising transparency at LHC, same parameter fits both RHIC and LHC, but Glauber + Bjorken longitudinal expansion background can be more realistic.

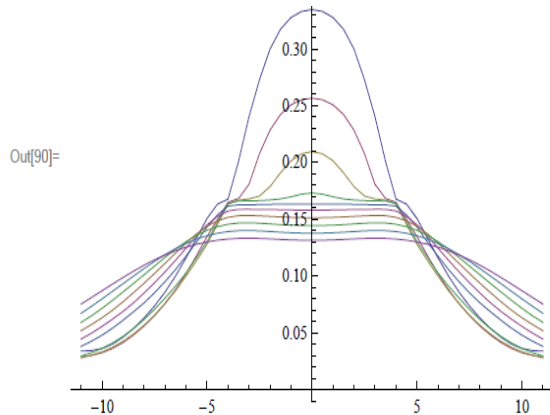
CUJET2.0 = rcDGLV + Elastic + 2+1D Viscous Hydro



T. Renk, H. Holopainen, U. Heinz and C. Shen, PRC 83, 014910 (2011)

C. Shen, U. Heinz, P. Huovinen and H. Song, PRC 82, 054904 (2010)

H. Song and U. Heinz, PRC 78, 024902 (2008)



❖ Couple rcDGLV to VISH 2+1D expanding QGP fluid fields ($T(x,t), v(x,t)$)

❖ RHIC Au+Au 200AGeV

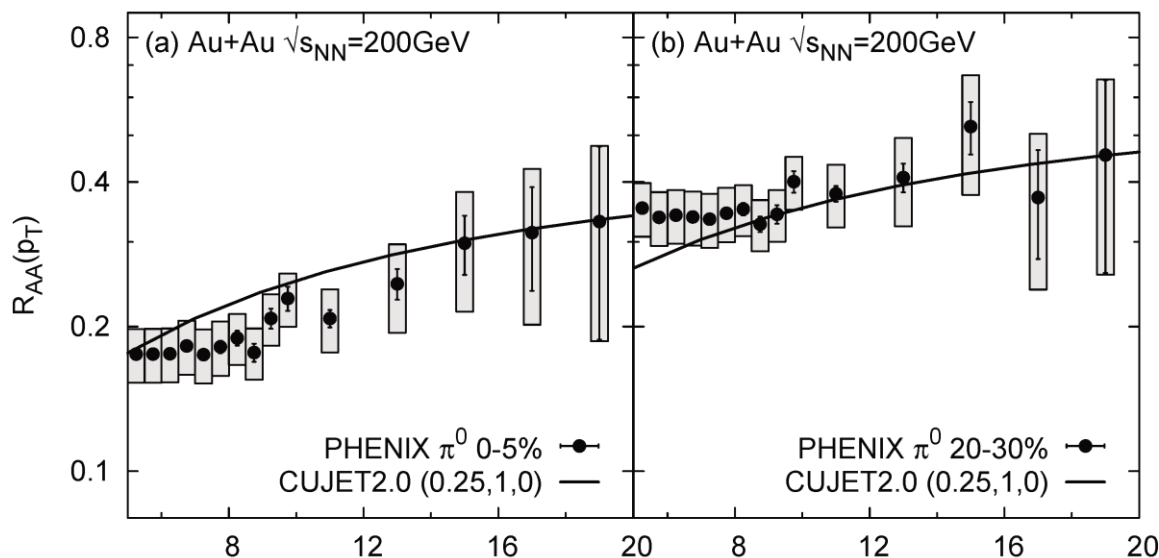
- Equation of State: s95p-PCE
- Initial Condition: MC-Glauber
- $\eta/s=0.08$
- Initial Time: 0.6fm/c
- Cooper-Frye freeze-out temperature: 120MeV

❖ LHC Pb+Pb 2.76ATeV

- Equation of State: s95p-PCE
- Initial Condition: MC-Glauber
- $\eta/s=0.08$
- Initial Time: 0.6fm/c
- Cooper-Frye freeze-out temperature: 120MeV

❖ Initial conditions for the hydro evolution are adjusted to roughly reproduce experimental pion and proton spectra from the 5% most central 200 AGeV Au+Au collisions

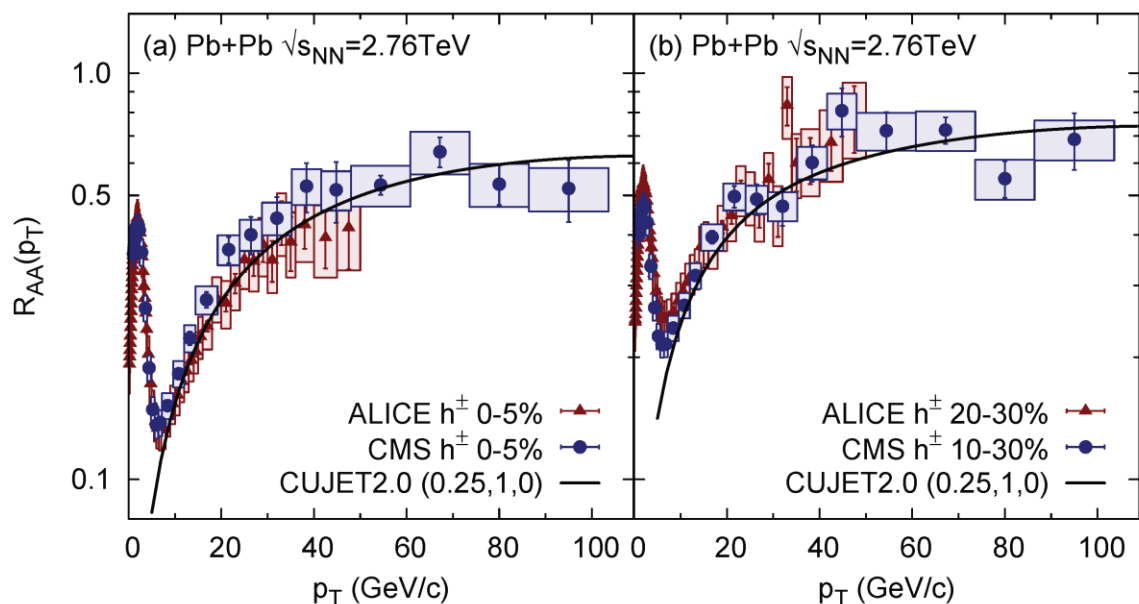
CUJET2.0 Result: R_{AA} at RHIC and LHC



❖ $(\alpha_{max}, f_E, f_M) = (0.25, 1, 0)$

❖ The pion R_{AA} is compatible with both RHIC and LHC data for central and mid-central collisions

➤ The same choice of running coupling but with a different medium evolution background can still explain the surprising transparency at LHC

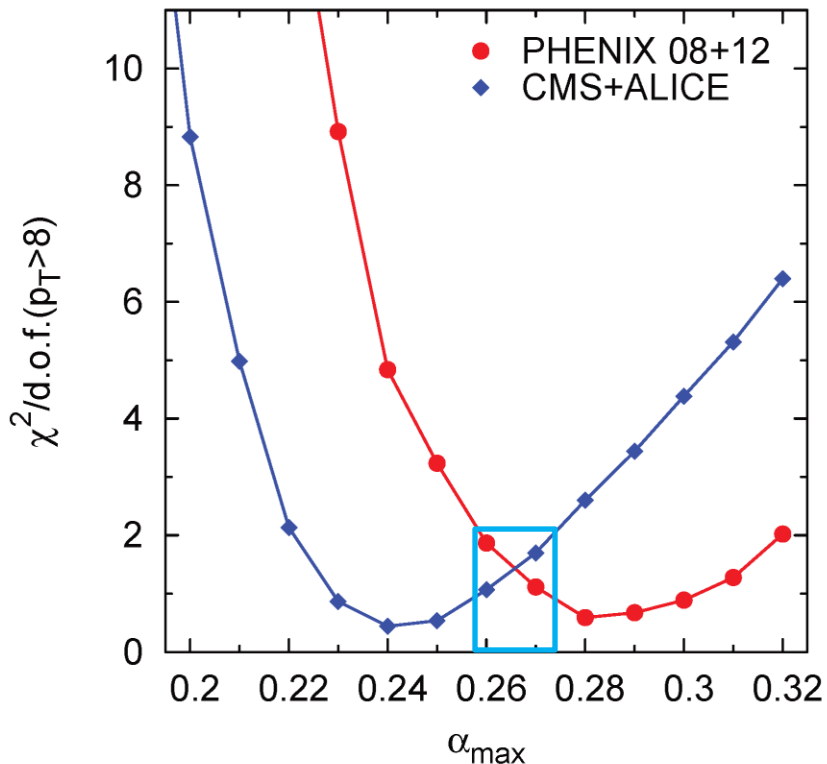
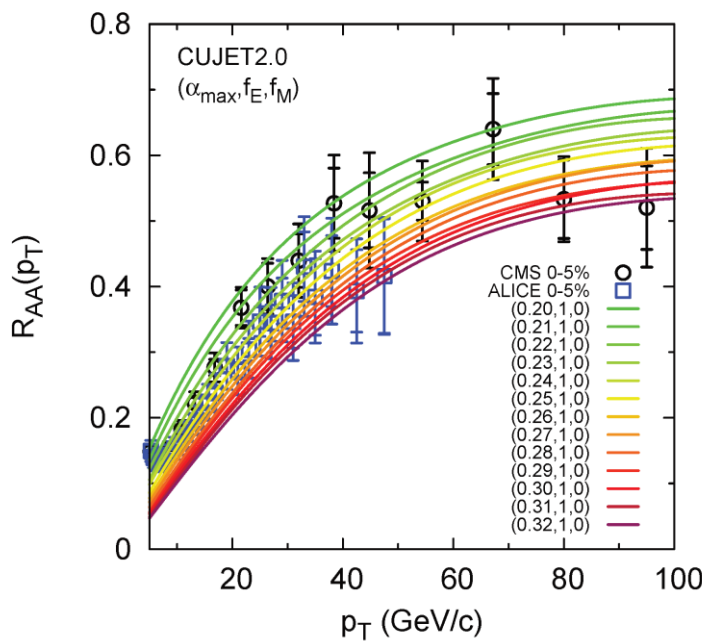
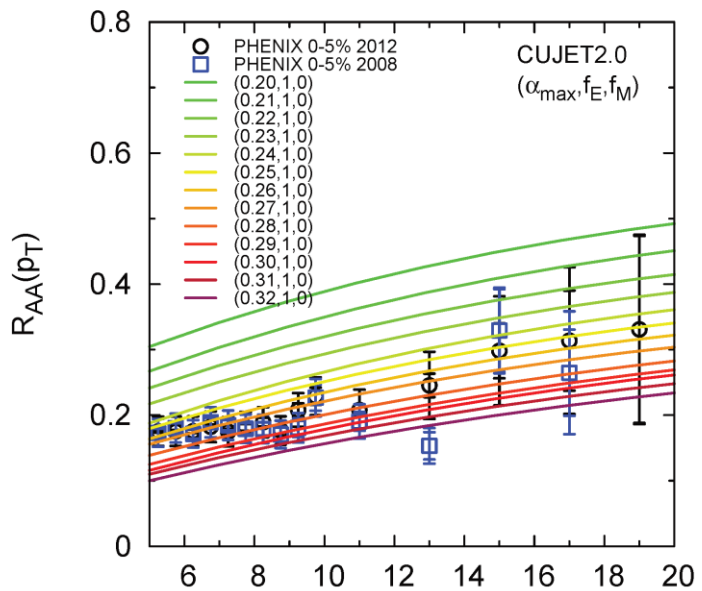


❖ Clearer tendency of flattening out at high p_T

❖ The coupling strength significantly decreases with an expanding transverse medium comparing to the static case

➤ Although density is smaller in VISH2+1 comparing to Glauber, longer path length contributes more to jet medium interaction, results in more energy loss

$$\chi^2/d.o.f.$$



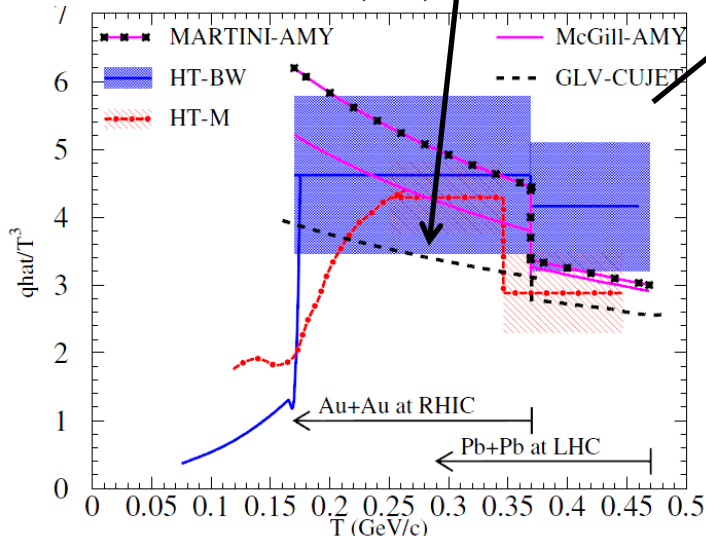
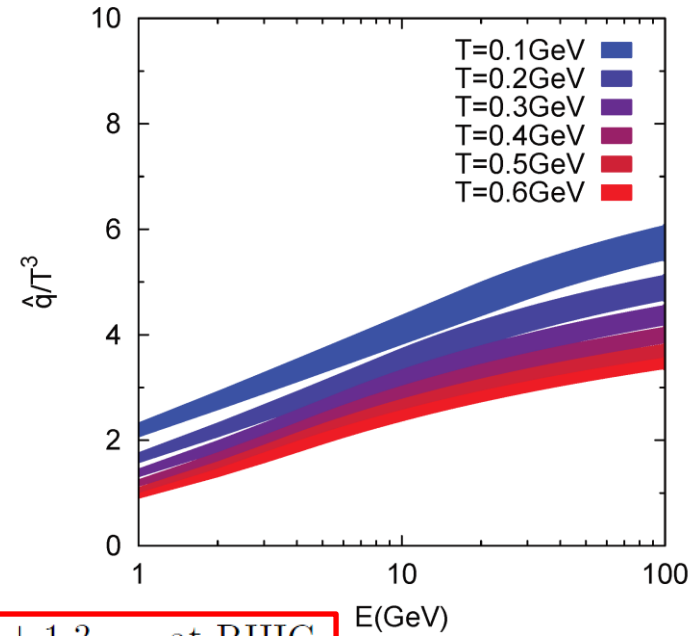
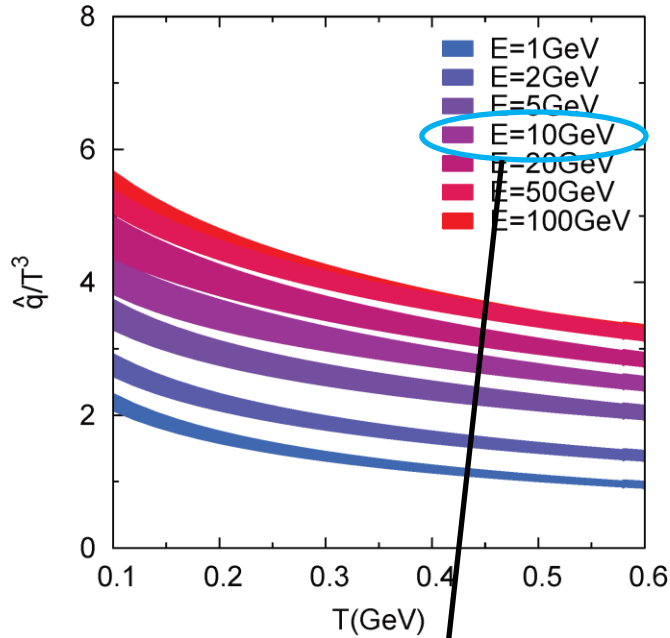
❖ Eikanol breaks down at low p_T , choose data above 8 GeV/c

❖ Allow 2 standard deviation, for HTL like $f_E = 1, f_M = 0$ model

➤ $\alpha_{max} = 0.26 \pm 0.01$

Jet Transport Coefficient

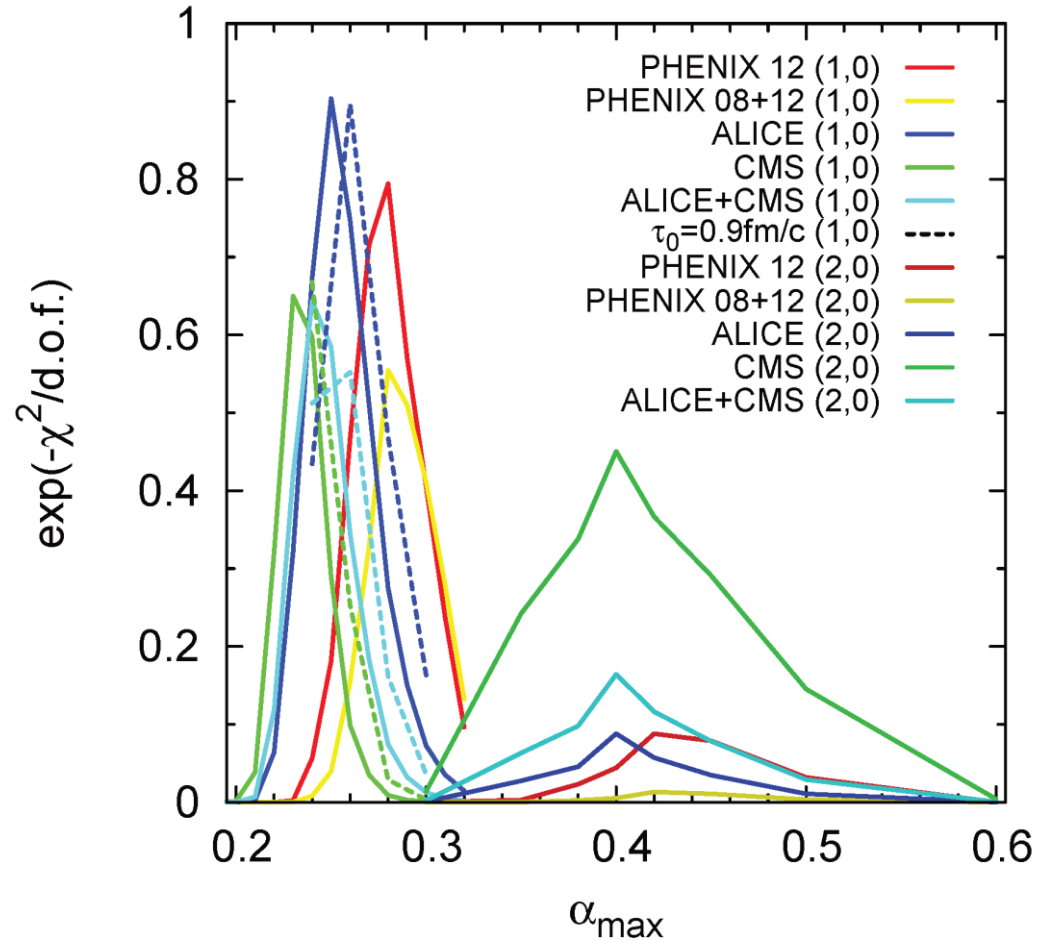
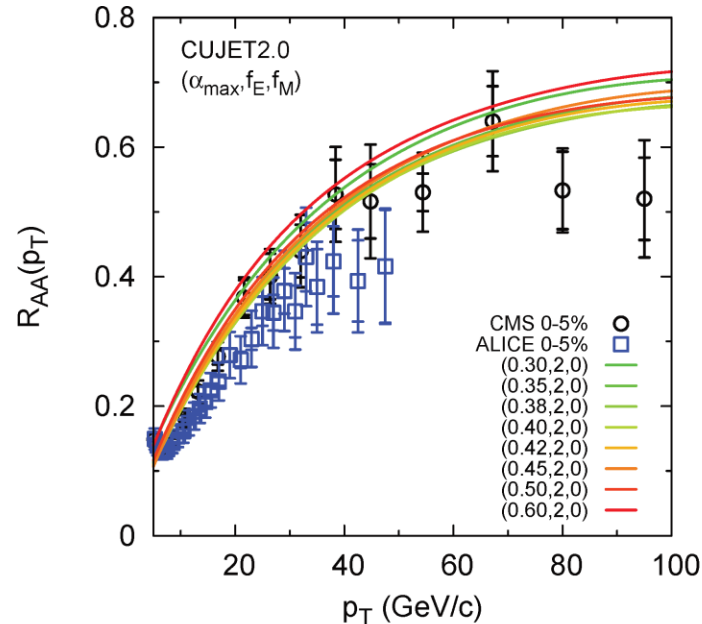
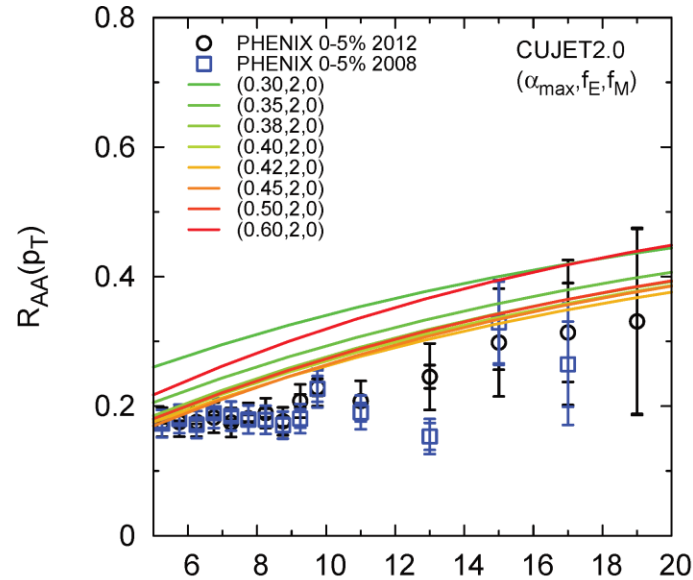
$$\hat{q}(E, T; \alpha_{max}, f_E, f_M) = \int dq^2 q^2 d\sigma / dq^2 \rho$$



$$\frac{\hat{q}}{T^3} \approx \begin{cases} 4.5 \pm 1.3 & \text{at RHIC,} \\ 3.7 \pm 1.4 & \text{at LHC.} \end{cases}$$

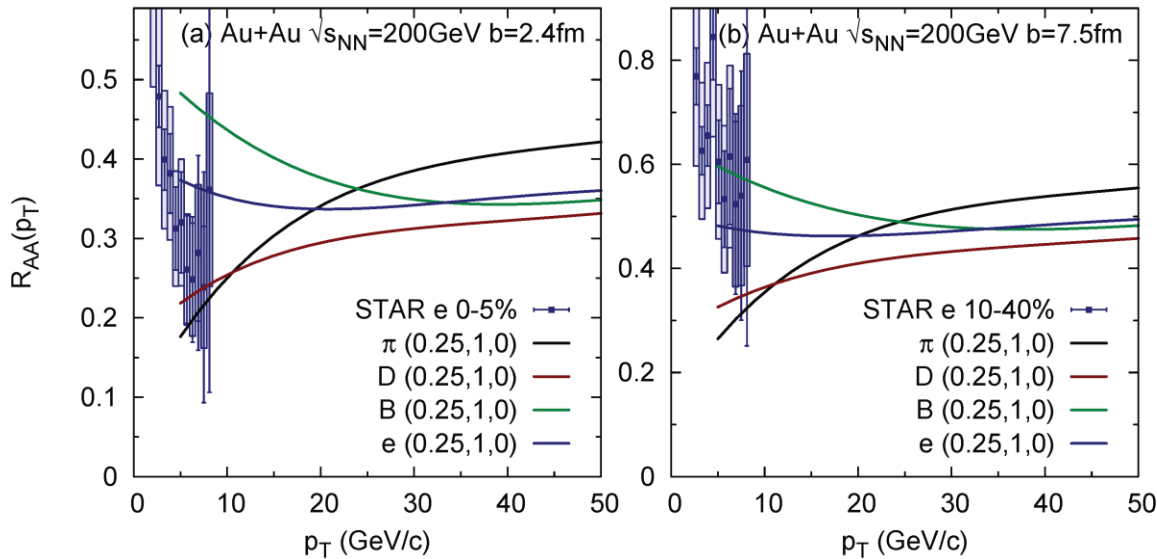
- ❖ At fixed initial energy, CUJET2.0's \hat{q}/T^3 decreases as increasing temperature
 - Within the above range at RHIC and LHC temperature
- ❖ At fixed temperature, \hat{q}/T^3 decreases as decreasing initial energy
 - $\eta/s = 1.6T^3/\hat{q}$ increases when lowering p_T at soft regime
 - Discrepancy: bulk flow suggests strongly coupled near “perfect fluidity” for $p_T < 2$ GeV/c, while hard jet probes suggest weak jet medium interactions $p_T > 10$ GeV/c.
 - CUJET2.0 combines bulk and jet, but is not able to bridge the discrepancy.

Non-HTL Scenario



- ❖ In the non-HTL model $f_E = 2$, $f_M = 0$, when increasing coupling strength, energy loss first increase then decrease
- ❖ RHIC+LHC data prefers HTL $\mu \sim gT$ rather than lattice like non-HTL scenario

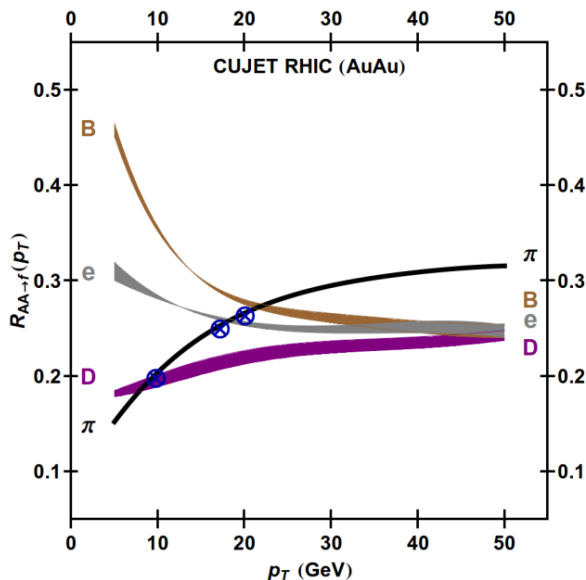
CUJET2.0 Result: Heavy Flavor at RHIC



❖ CUJET2.0 explains the non-photonic electron spectrum at STAR

❖ At low p_T , charm and pion mixed together, while beauty is well-separated

➤ Beauty is the key constraint on model parameter space



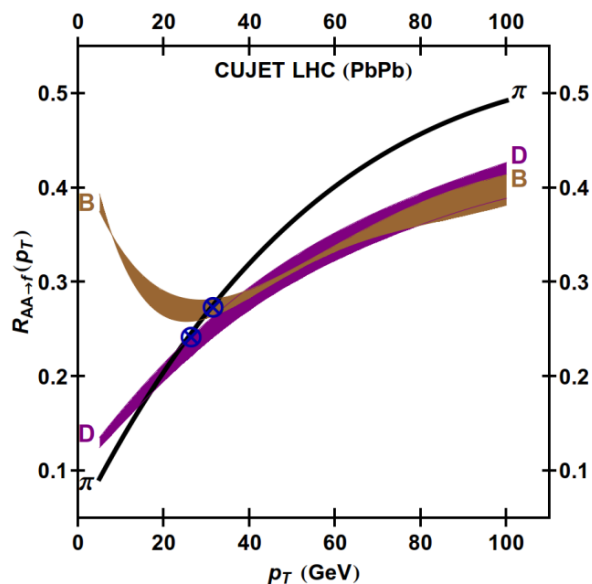
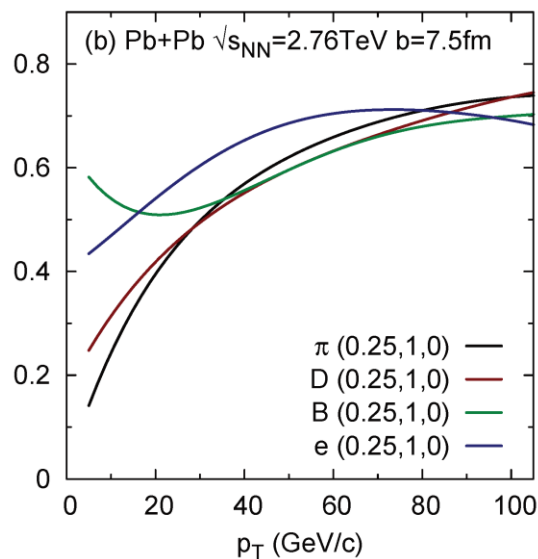
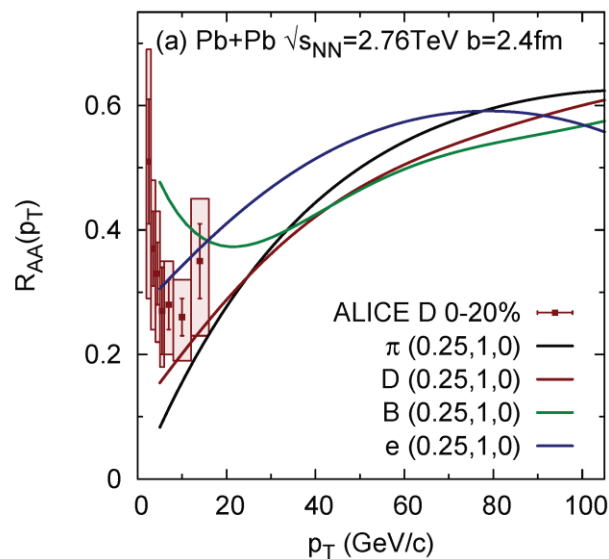
Buzzatti, Gyulassy, PRL (2012)

❖ Left: CUJET1.0 flavor tomography result (with fixed coupling $\alpha_s = 0.3$ HTL)

❖ Level crossing from Bjorken expansion CUJET1.0 and viscous hydro coupled CUJET2.0 (0.25, 1, 0) occurs at approximately the same p_T

➤ Open question: currently no flavor dependence in the running coupling of CUJET2.0

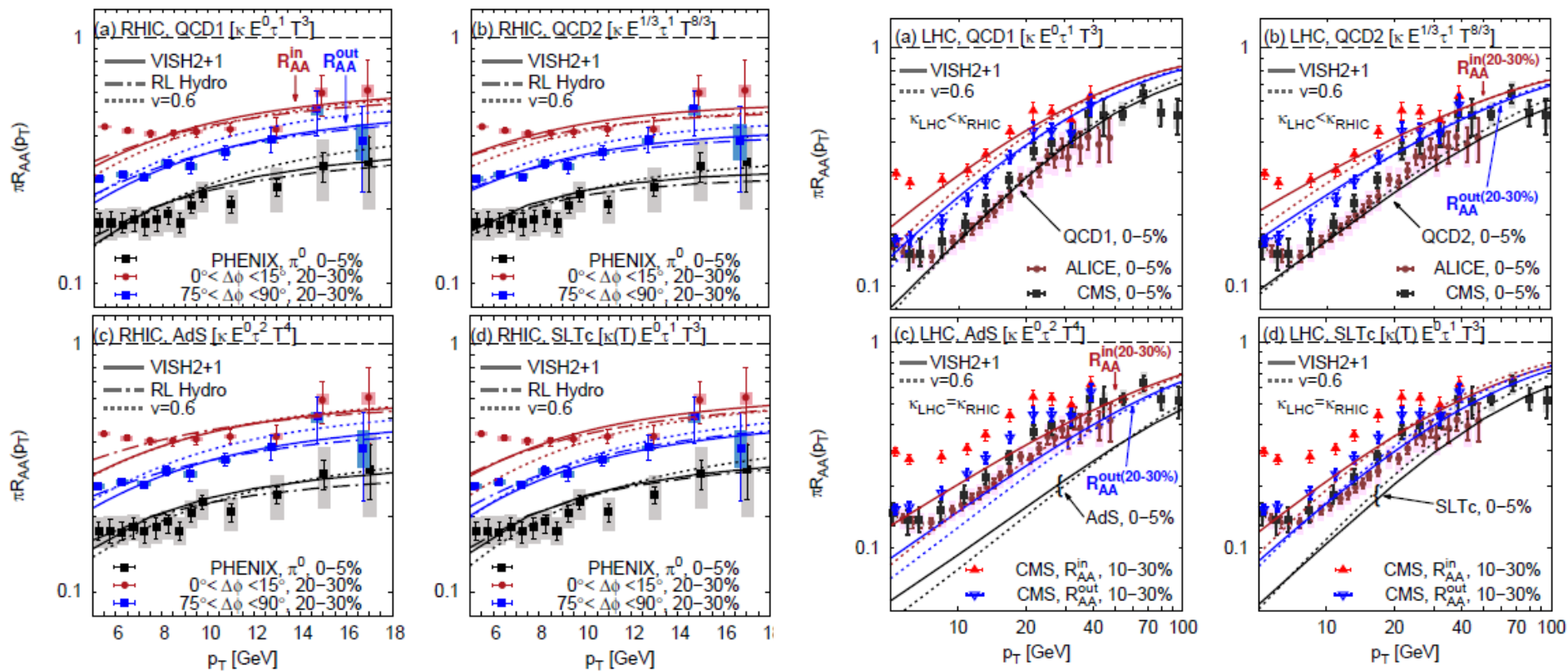
CUJET2.0 Result: Heavy Flavor at LHC



Buzzatti, Gyulassy, PRL (2012)

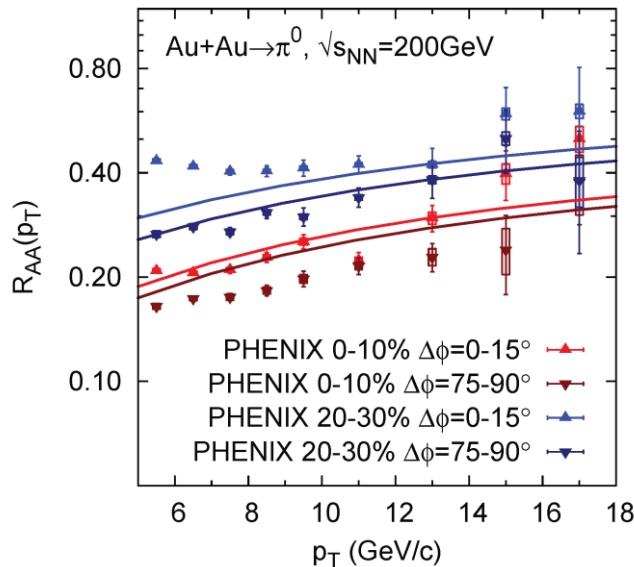
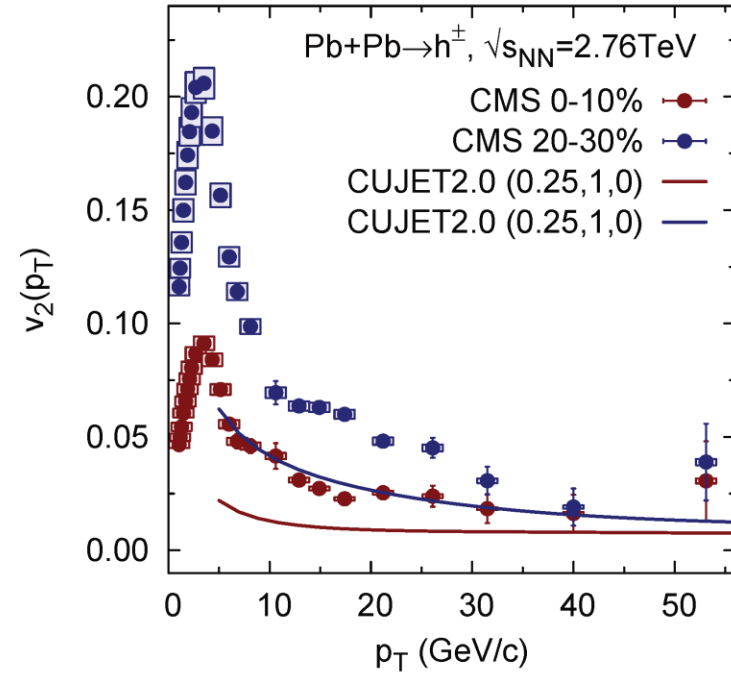
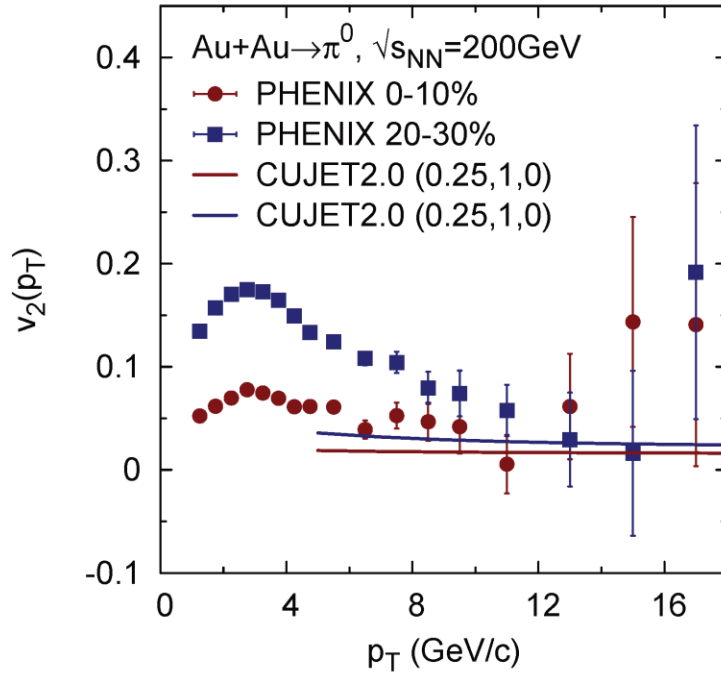
- ❖ CUJET2.0 explains the average D meson spectrum at ALICE
- ❖ At low p_T , charm and pion are more clearly mixed together
 - Beauty is still the key constraint on model parameter space
- ❖ $e > B > D$ at mid p_T
 - $B \rightarrow D \rightarrow e$ process may have significant contribution
- ❖ Electron R_{AA} decreases at high p_T
 - Fragment from unphysical regime of heavy quark spectrum
- ❖ Left: CUJET1.0 flavor tomography result (with fixed coupling $\alpha_s = 0.3$ HTL)
- ❖ Level crossing from Bjorken expansion CUJET1.0 and viscous hydro coupled CUJET2.0 (0.25, 1, 0) occurs at approximately the same p_T

Simultaneously fit R_{AA} and v_2



- ❖ B. Betz and M. Gyulassy, arXiv:1305.6458
 - QCD1 \rightarrow rcCUJET1.0; QCD2 \rightarrow fcCUJET1.0; AdS \rightarrow fixed t'Hooft conformal falling string; SLTc \rightarrow Shuryak-Liao assuming T_c dominated
 - VISH2+1-Shen,Heinz,Song; RL-Romatschke,Luzum
- ❖ D. Molnar and S. Deke, arXiv:1305.1046
 - R_{AA} and v_2 cannot be satisfied with the same set of parameters in MPC+GLV

CUJET2.0 Result: v_2



- ❖ v_2 is 50% lower at both RHIC and LHC
- ❖ Azimuthal Asymmetry $\approx (\text{dE/dx Model})/2 + (\text{spacetime bulk hydro 2+1D flow})/2$ (“Renk’s Lemma”)
- ❖ Depend on a complex interplay between details of microscopic $p_T > 10$ GeV/c jet dE/dx (abc) and details of the spacetime evolution of the bulk soft $p_T < 2$ GeV/c sQGP (IC, η/s , τ_0)
- ❖ Radiative energy loss fluctuation may smear out the large asymmetry from hydro
- ❖ v_2 is the elephant in the room!

Summary and Outlook

Summary


- ❖ CUJET offers a reliable and flexible model which is able to compute leading hadron jet energy loss and compare directly with data.
- ❖ With dynamical scattering effect and elastic energy loss included, CUJET1.0's electron spectrum is consistent within uncertainties of data.
- ❖ Running coupling is in simultaneous agreement with RHIC and LHC data.
- ❖ CUJET2.0 = rcDGLV + Elastic + VISH2+1. RHIC+LHC data prefers HTL CUJET2.0 model.
- ❖ Novel level crossing pattern of flavor dependent R_{AA} is found. Heavy flavor especially beauty is the key constraint on model space.
- ❖ Jet transport coefficient from the CUJET2.0 result suggests a weakly-coupled jet-medium interaction, different from bulk like sQGP.
- ❖ Long standing puzzle of simultaneously fit of R_{AA} and v_2 correlations remains!

Outlook

- ❖ Extrapolate effective running coupling and scattering potential from lattice QCD data on non-perturbative $V(r,T)$, and examine whether lattice QCD predicts the correct jet medium physics near T_c .
- ❖ Explore Shuryak-Liao magnetic monopole enhancement in CUJET2.0 framework for larger asymmetry.
- ❖ Study absolute particle production spectrums rather than ratios.
- ❖ Test CUJET2.0 predicted jet flavor and azimuthal tomography against all RHIC vs LHC data systematics.

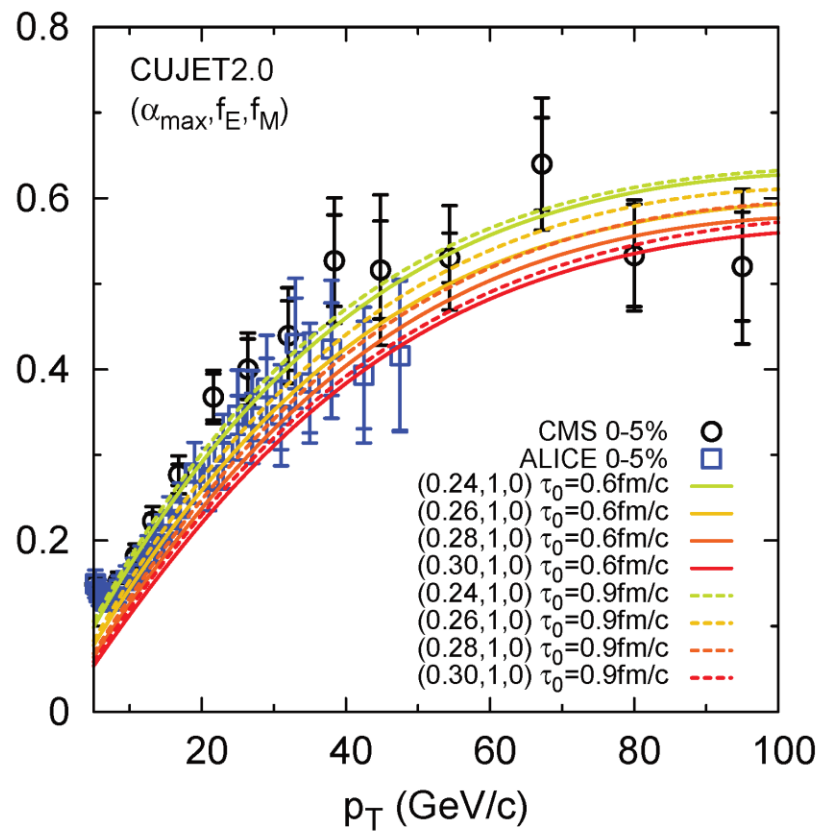
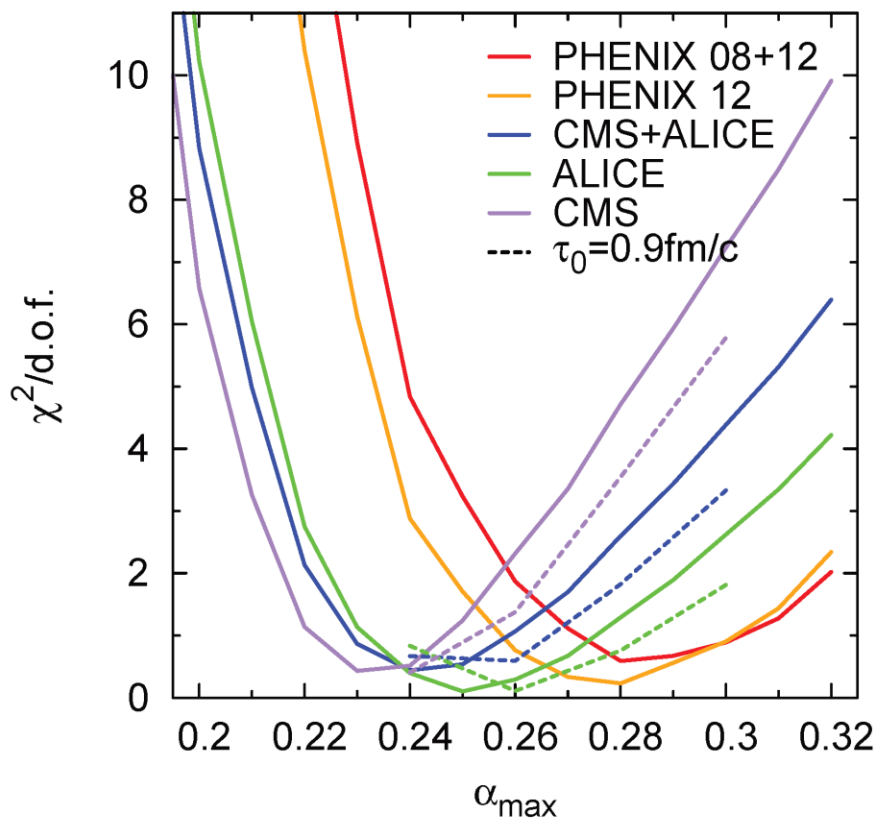
BACKUP

Systematic errors

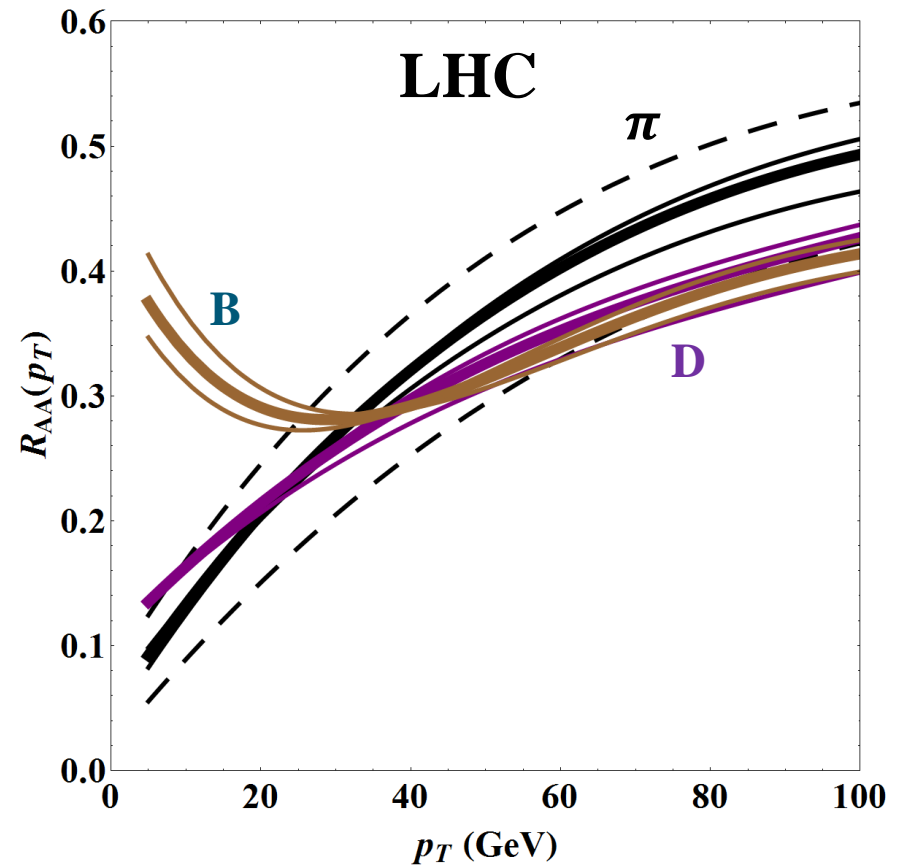
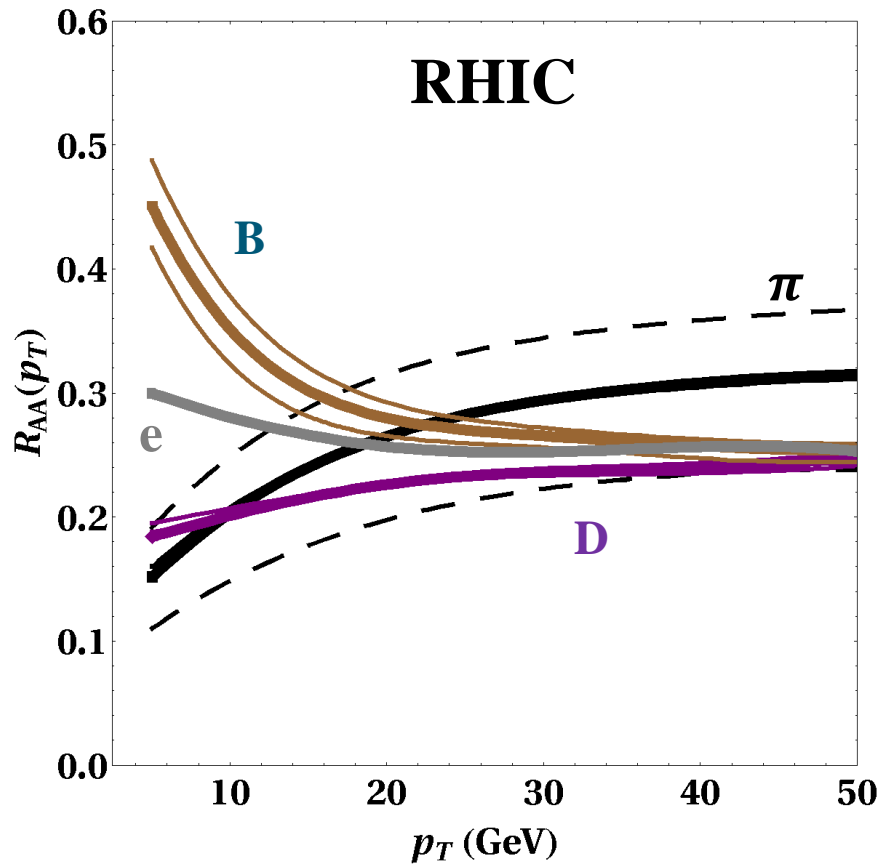
- ❖ Opacity order expansion
 - ❖ Choice of interaction potential
 - ❖ Pre-equilibrium phase
 - **ALSO:**
 - ❖ pp Spectra
 - ❖ Running coupling scales
- 

1. **One free parameter in the model: α_s^{eff}**
2. **Fit α_s^{eff} to 10GeV RHIC Pion data $\alpha_s^{eff} \approx 0.3 \pm 10\%$**
3. **All other predictions are fully constrained**

Initial Time



τ_0 sensitivity



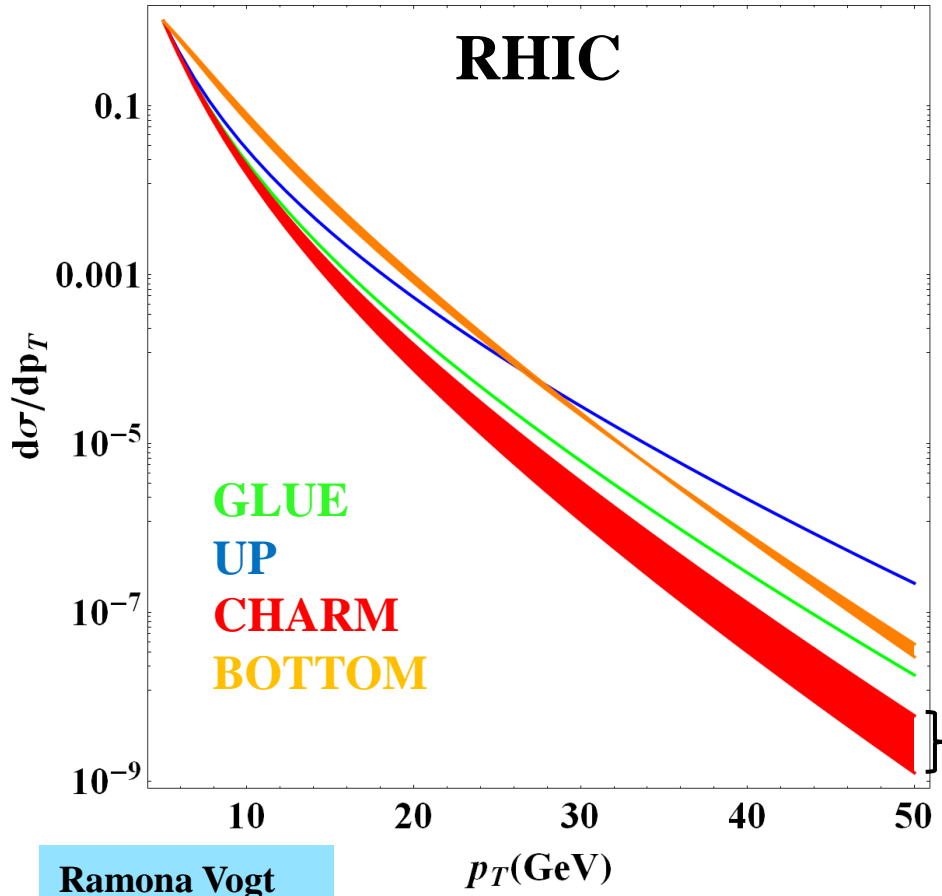
THICK: Linear with $\alpha_s = 0.3$

THIN: Divergent with $\alpha_s = 0.27$ or Freestreaming with $\alpha_s = 0.325$

DAHSED: Divergent or Freestreaming with $\alpha_s = 0.3$

Initial p QCD spectra

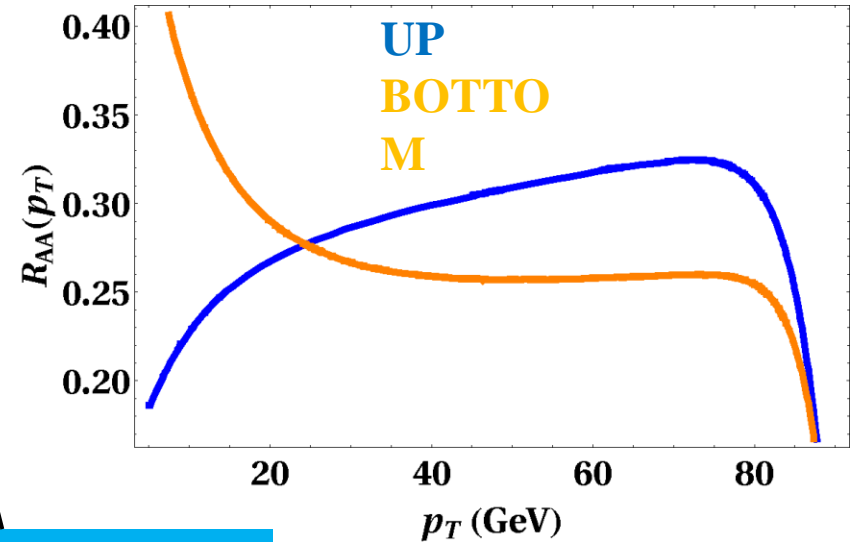
Initial quark production spectra



NLO-FONLL uncertainty

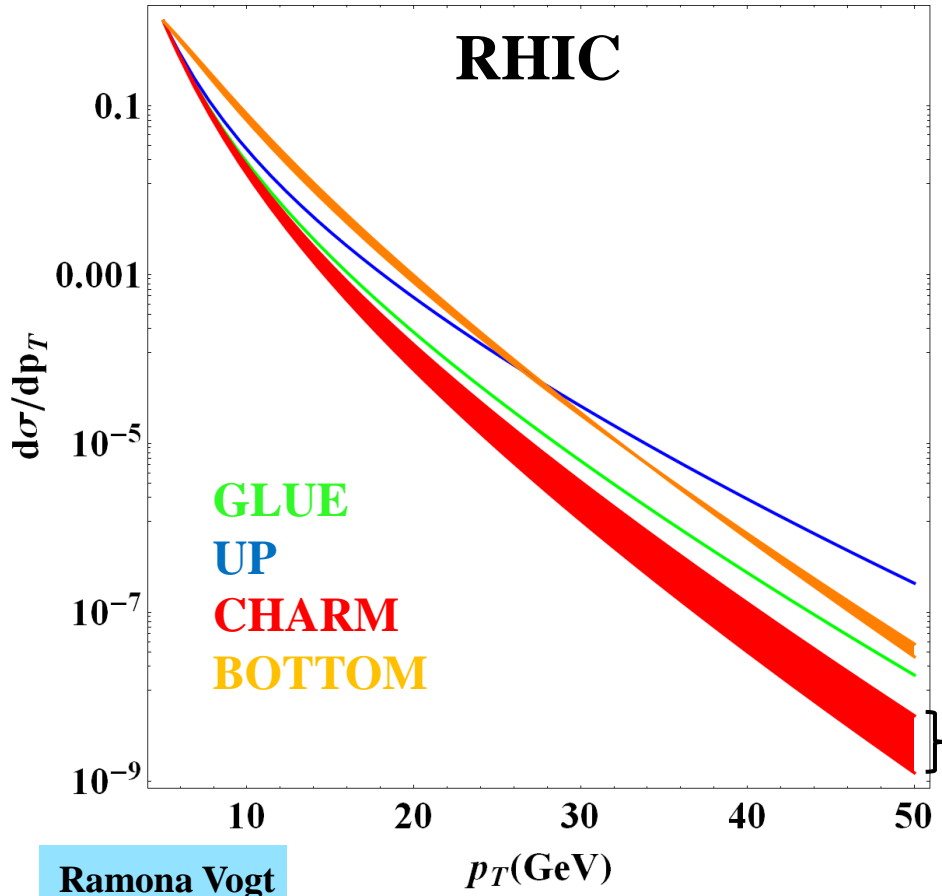
Competing effects between increased density and harder production spectra

- **RHIC density and spectra**
- LHC density, RHIC spectra
- LHC density and spectra



Initial p QCD spectra

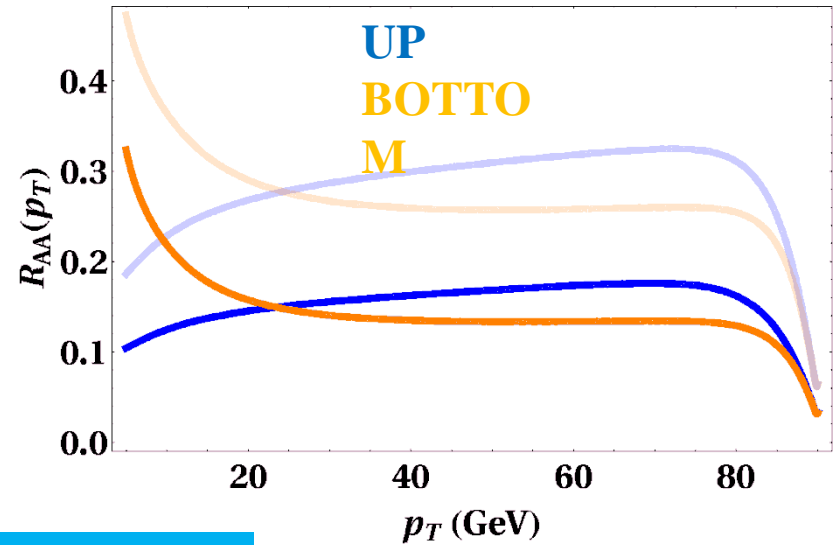
Initial quark production spectra



NLO-FONLL uncertainty

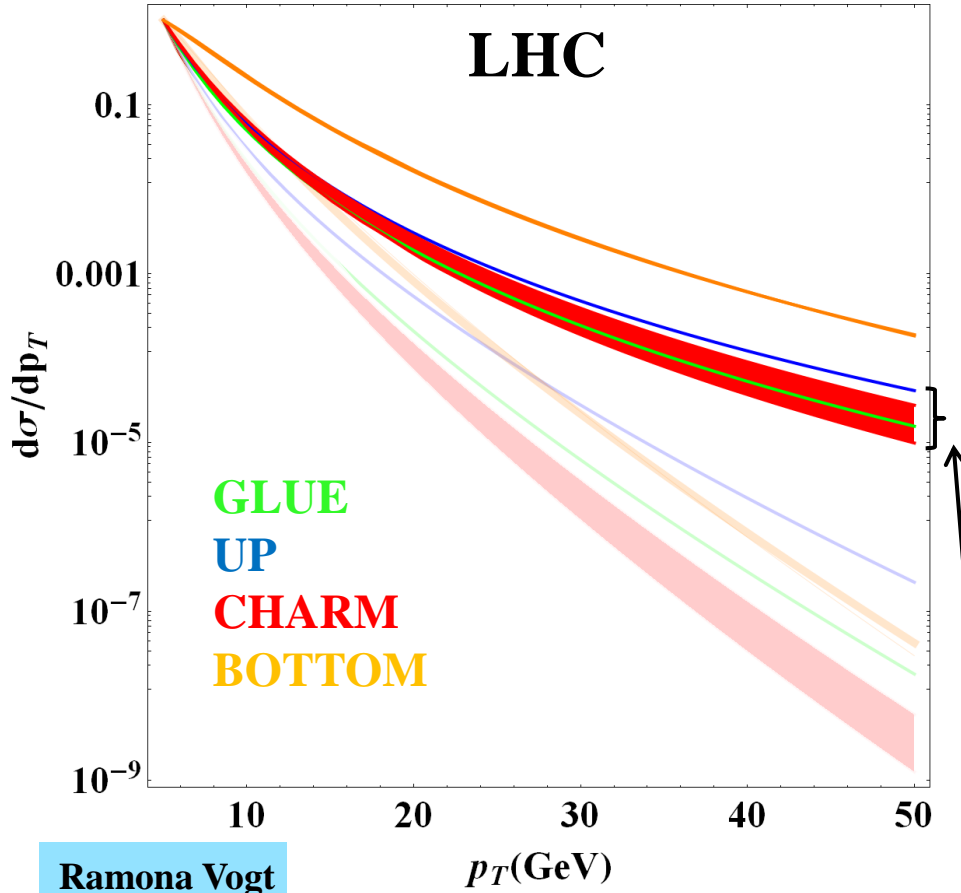
Competing effects between increased density and harder production spectra

- RHIC density and spectra
- LHC density, RHIC spectra
- LHC density and spectra



Initial p QCD spectra

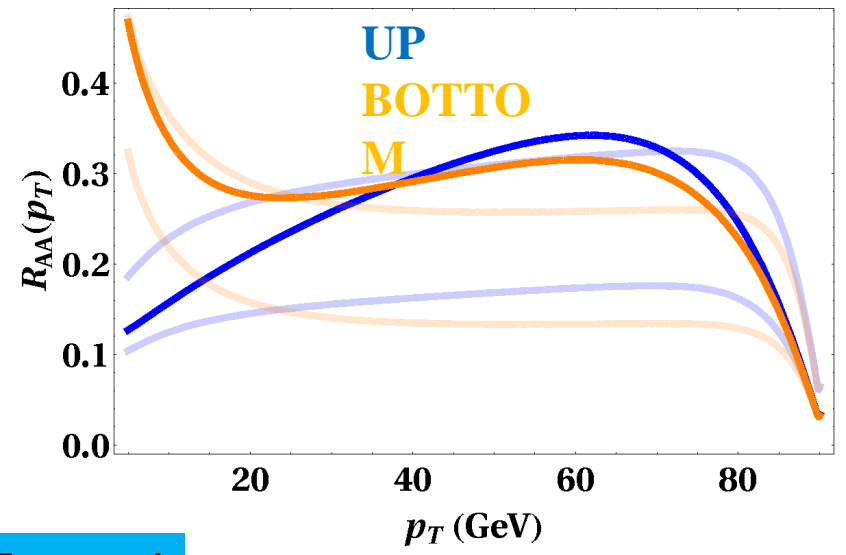
Initial quark production spectra



NLO-FONLL uncertainty

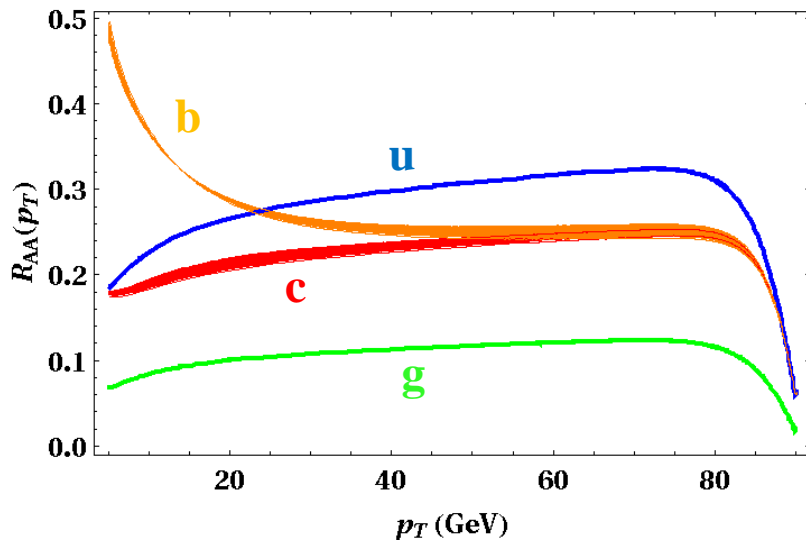
Competing effects between increased density and harder production spectra

- RHC density and spectra
- LHC density, RHC spectra
- **LHC density and spectra**

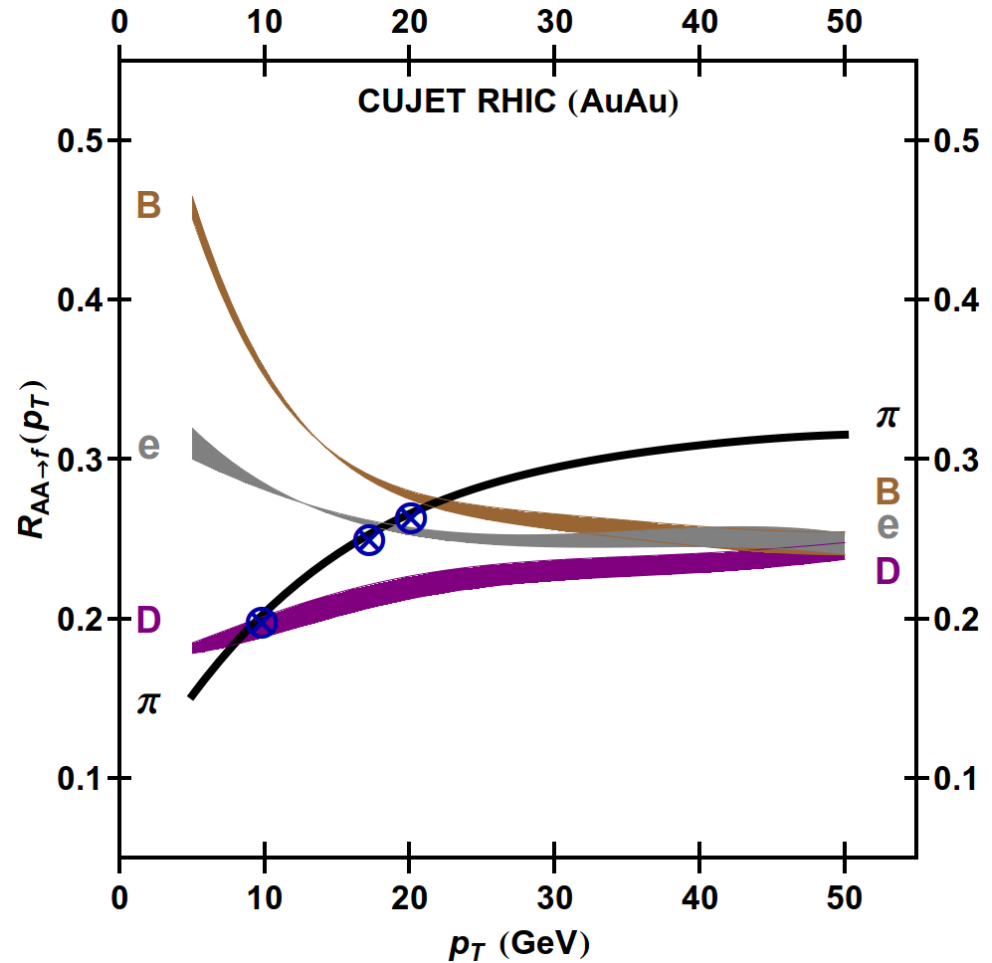


RHIC Results

0 – 5% centrality, $dNdy = 1000$, $\alpha_s = 0.3$, $\tau_0 = 1fm/c$



Inversion of R_{AA} flavor hierarchy at sufficiently high p_t



LHC Results

Parameters constrained by RHIC
 $dNdy = 2200$

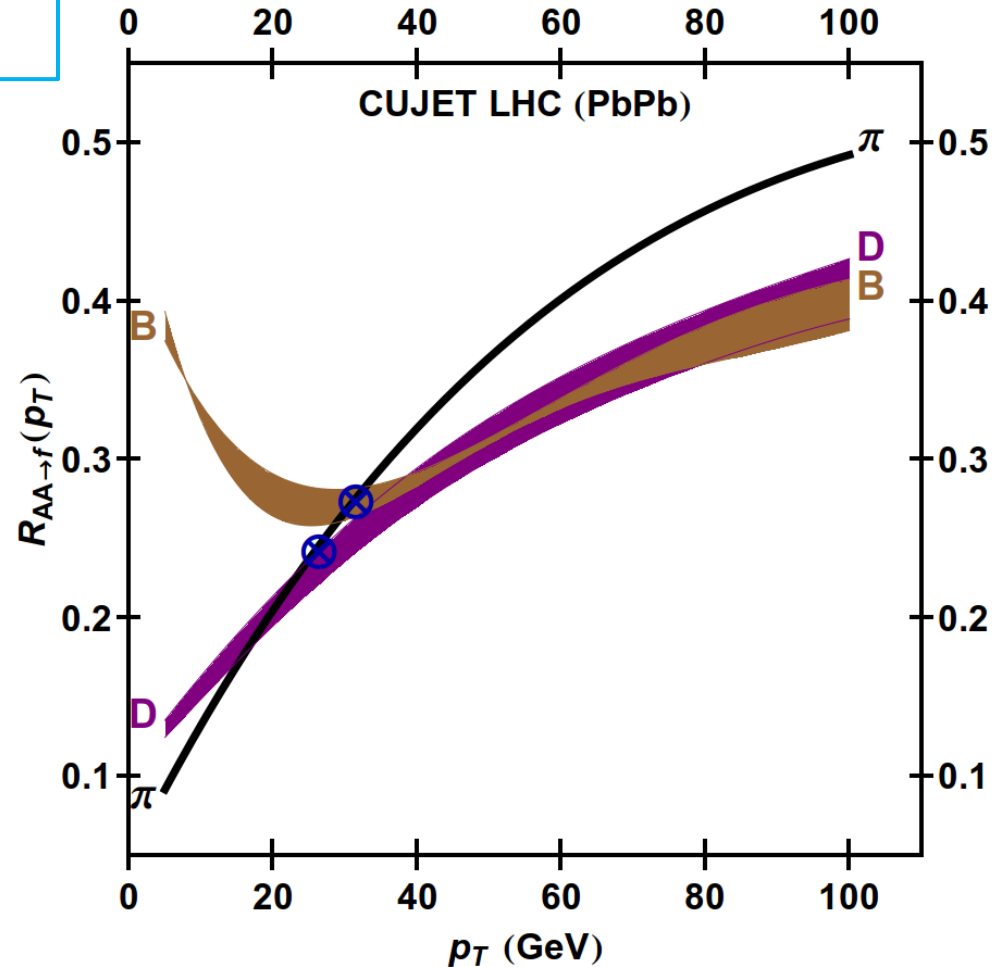
Competing effect between Energy loss ordering...

$$\Delta E(\text{light}) \approx \Delta E(c) > \Delta E(b)$$

...and pp Production spectra

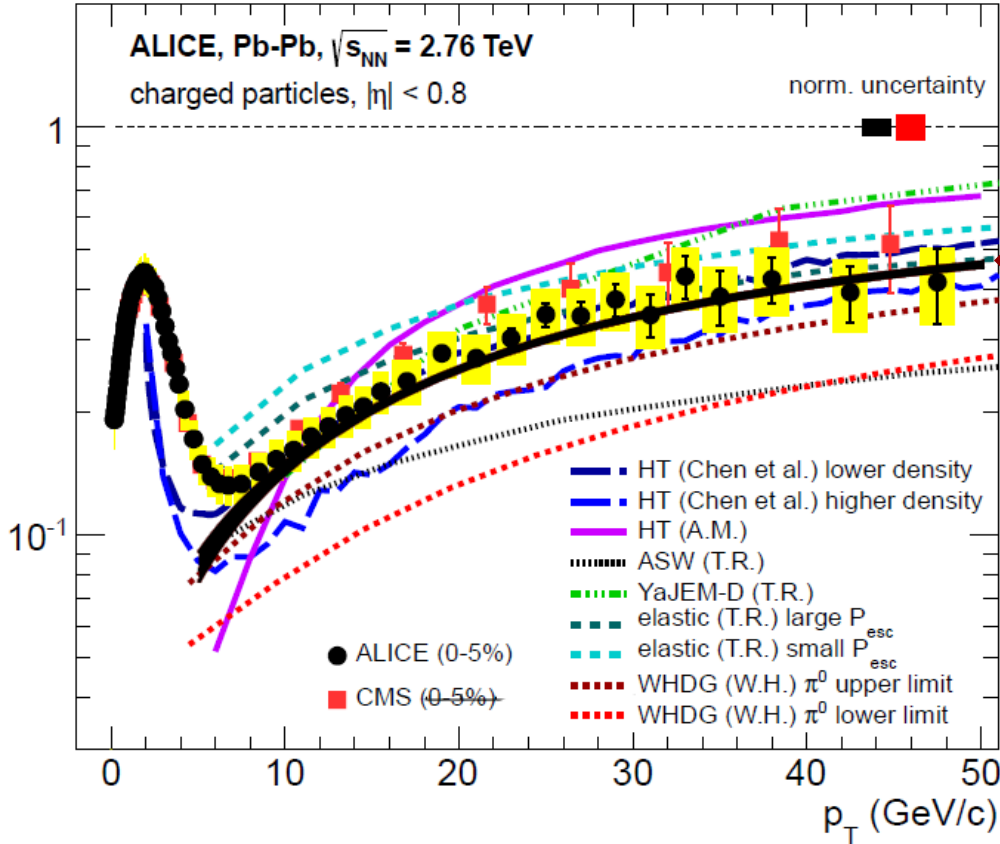
$d\sigma(c, b)$ harder than $d\sigma(\text{light})$

$$RAA \sim (1 - \Delta E/E)^{n-2}$$

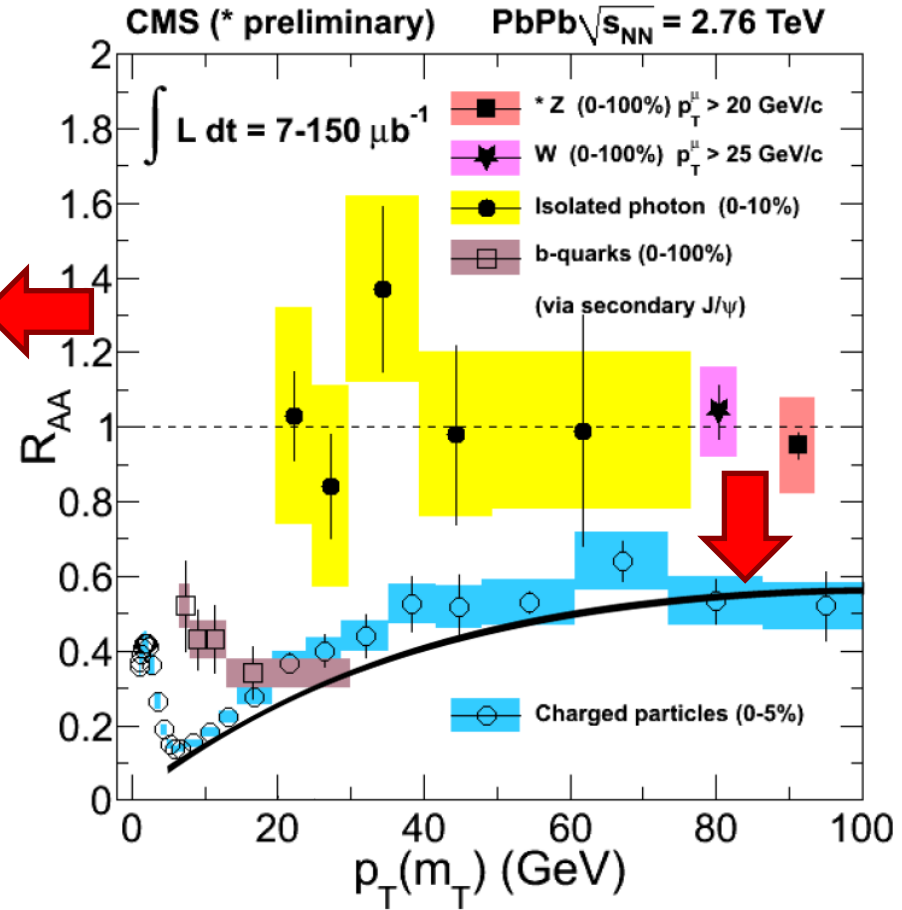


ALICE and CMS Pions

ALICE Collaboration

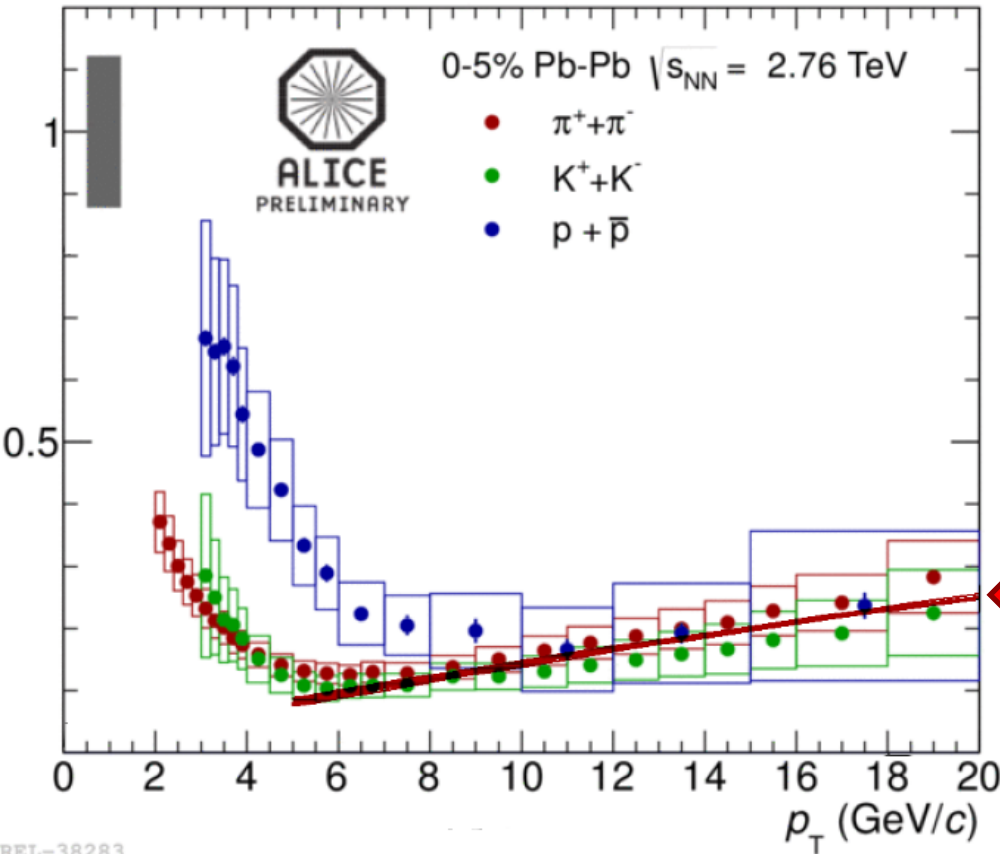


CMS Collaboration

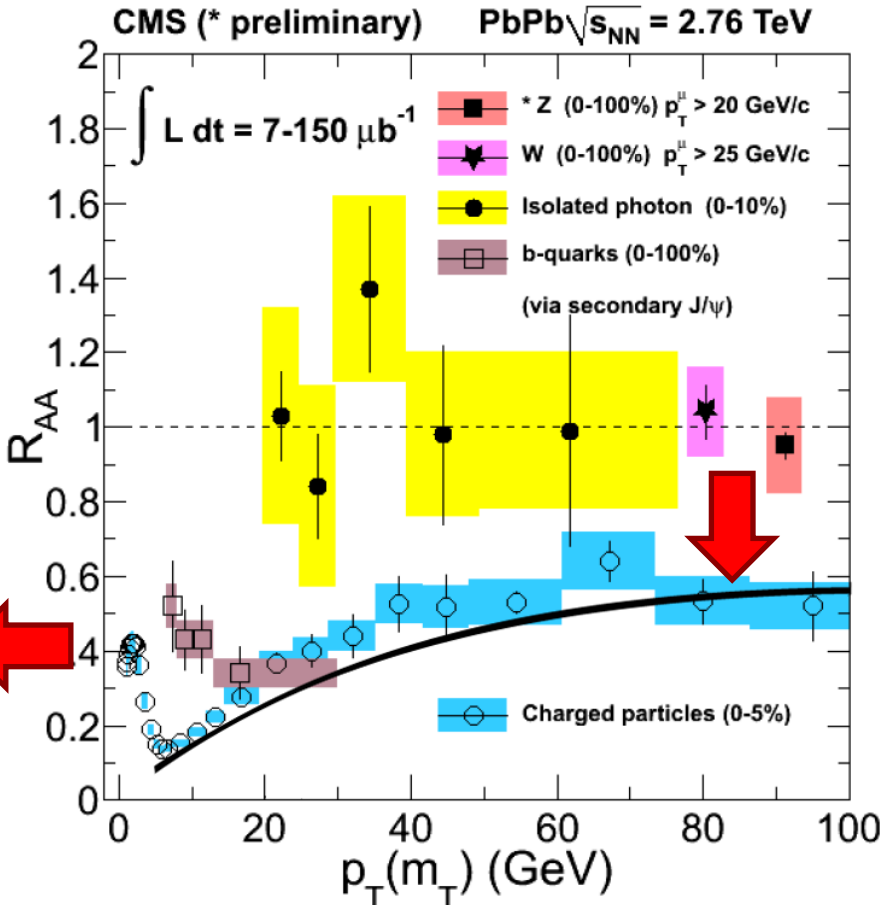


ALICE and CMS Pions

ALICE Collaboration

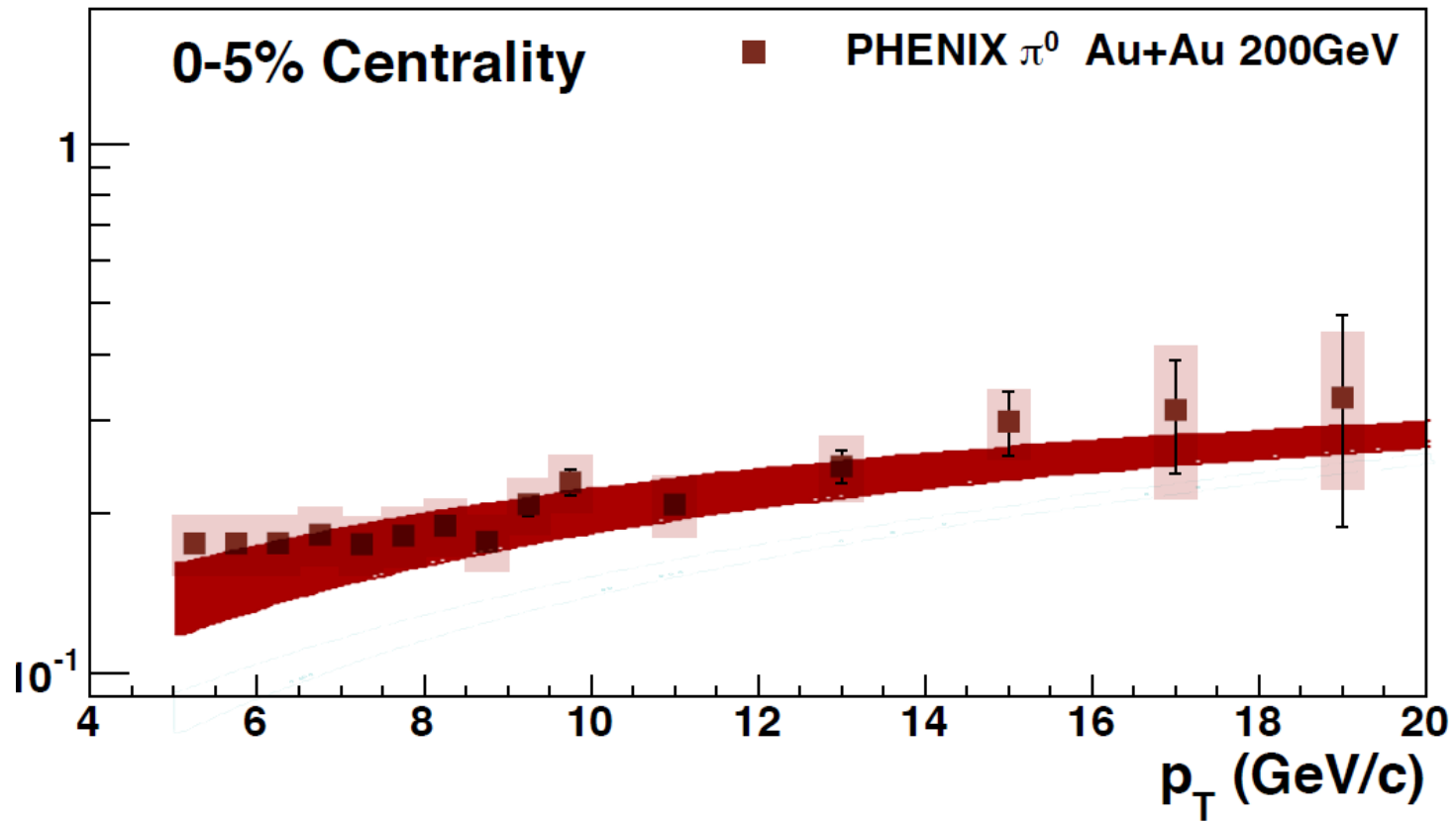


CMS Collaboration



PHENIX Pions

PHENIX Collaboration

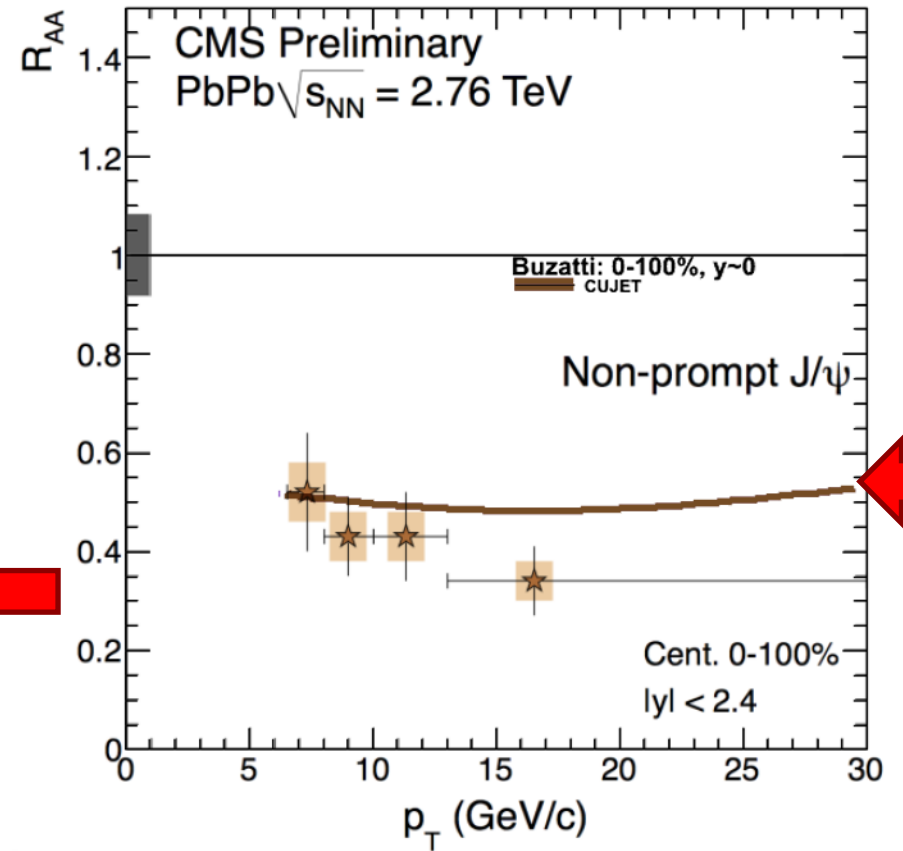
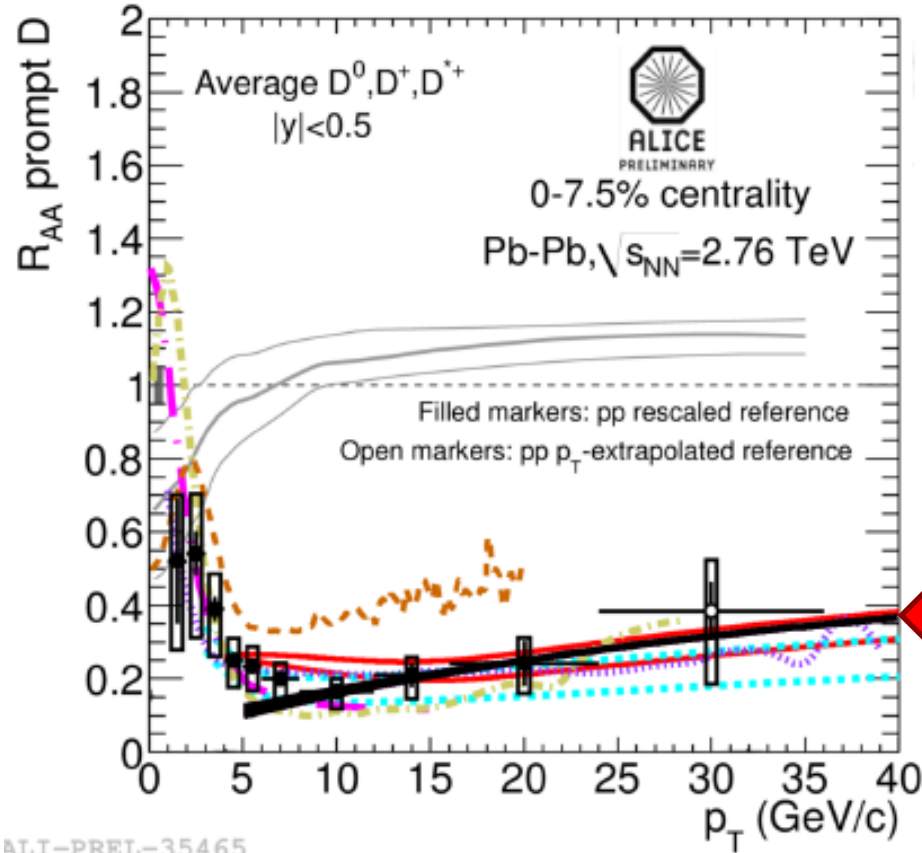


ALICE and CMS Heavy Flavors

ALICE Collaboration

CMS Collaboration

CMS-PAS HIN-12-014



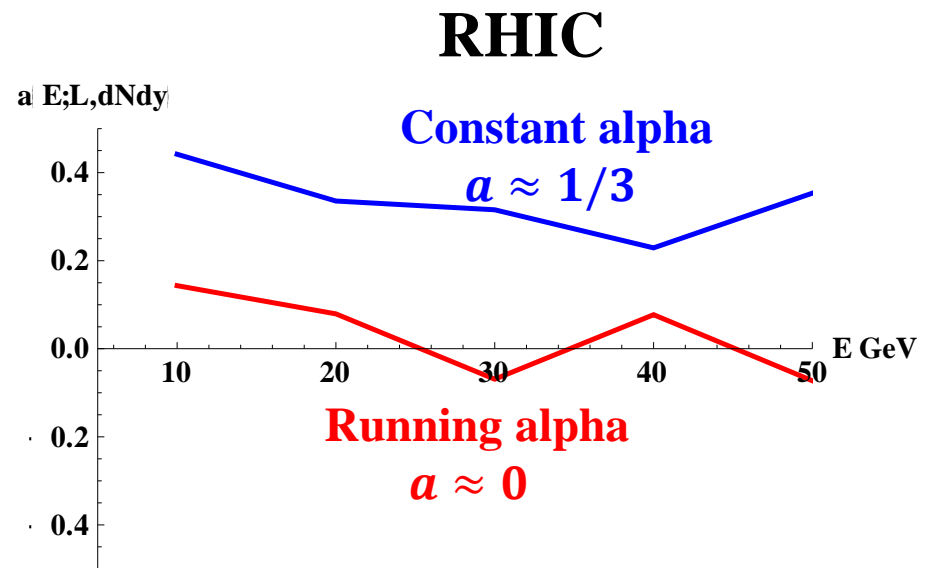
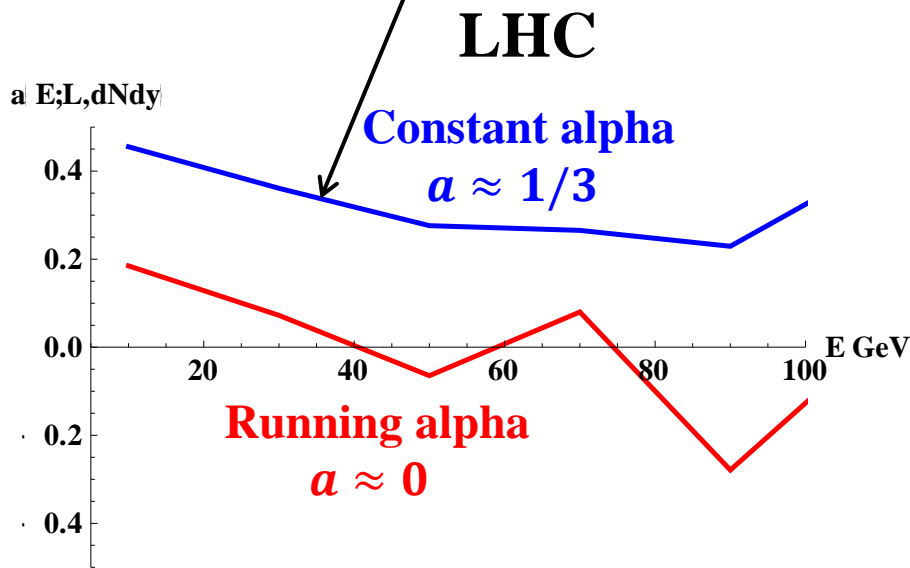
Energy loss

❖ Consider a simplified power law model for Energy loss:

$$\frac{\Delta E}{E} = \kappa E^{a-1} L^b \rho^c$$

W. A. Horowitz and M. Gyulassy, arXiv:1104.4958

B. Betz and M. Gyulassy, arXiv:1201.0218



Bjorken expansion

❖ The local thermal equilibrium is established at τ_0

$$s(\tau) = s_0 \frac{\tau_0}{\tau} \quad (\text{entropy equation})$$

$$s_0 \approx 3.6 \rho_0 = 3.6 \frac{1}{\pi R^2 \tau_0} \frac{dN}{dy} \quad \left(\frac{dN}{dy} \text{ is the observed rapidity density}\right)$$

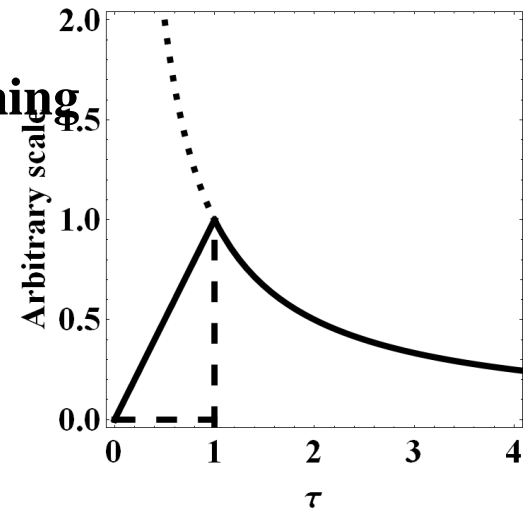
$$\rho_{QGP}(x_{\perp}, \tau) = \frac{1}{\tau_0} \frac{\rho_{part}(x_{\perp})}{N_{part}} \frac{dN}{dy} f\left(\frac{\tau}{\tau_0}\right)$$

MONOTONIC density dependence

❖ Before equilibrium

Temporal envelopes: linear, divergent, freestreaming

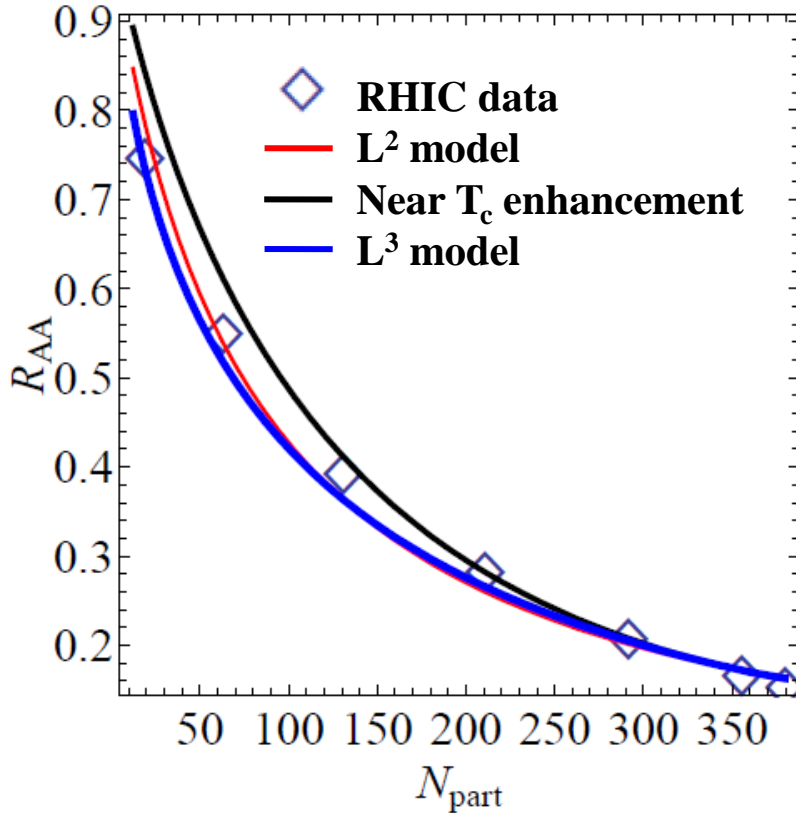
$$f\left(\frac{\tau}{\tau_0}\right) = \begin{cases} \frac{\tau}{\tau_0}, \frac{\tau_0}{\tau}, 0 & (\tau < \tau_0) \\ \frac{\tau_0}{\tau} & (\tau > \tau_0) \end{cases}$$



Magnetic monopoles

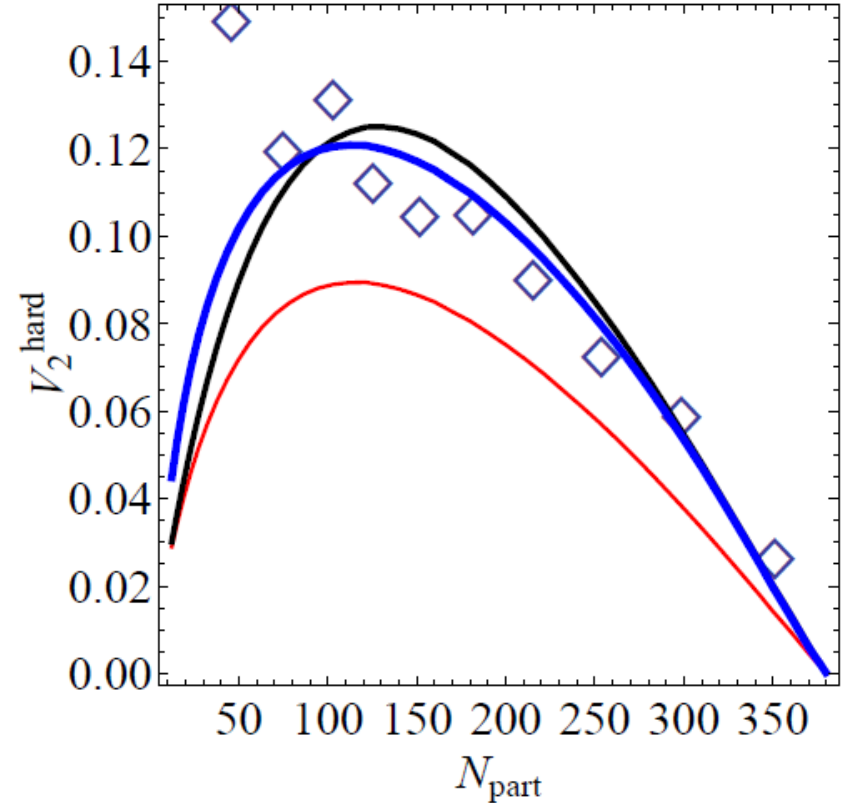
Magnetic monopole enhancement

- **Nonlinear density dependence near T_c**

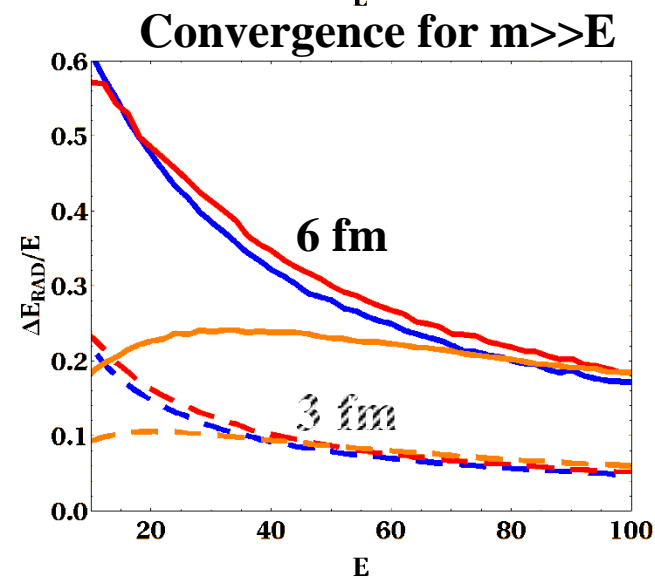
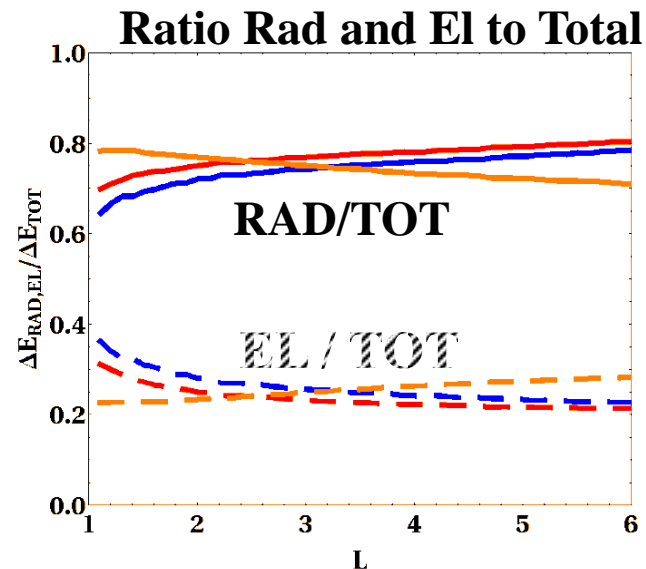
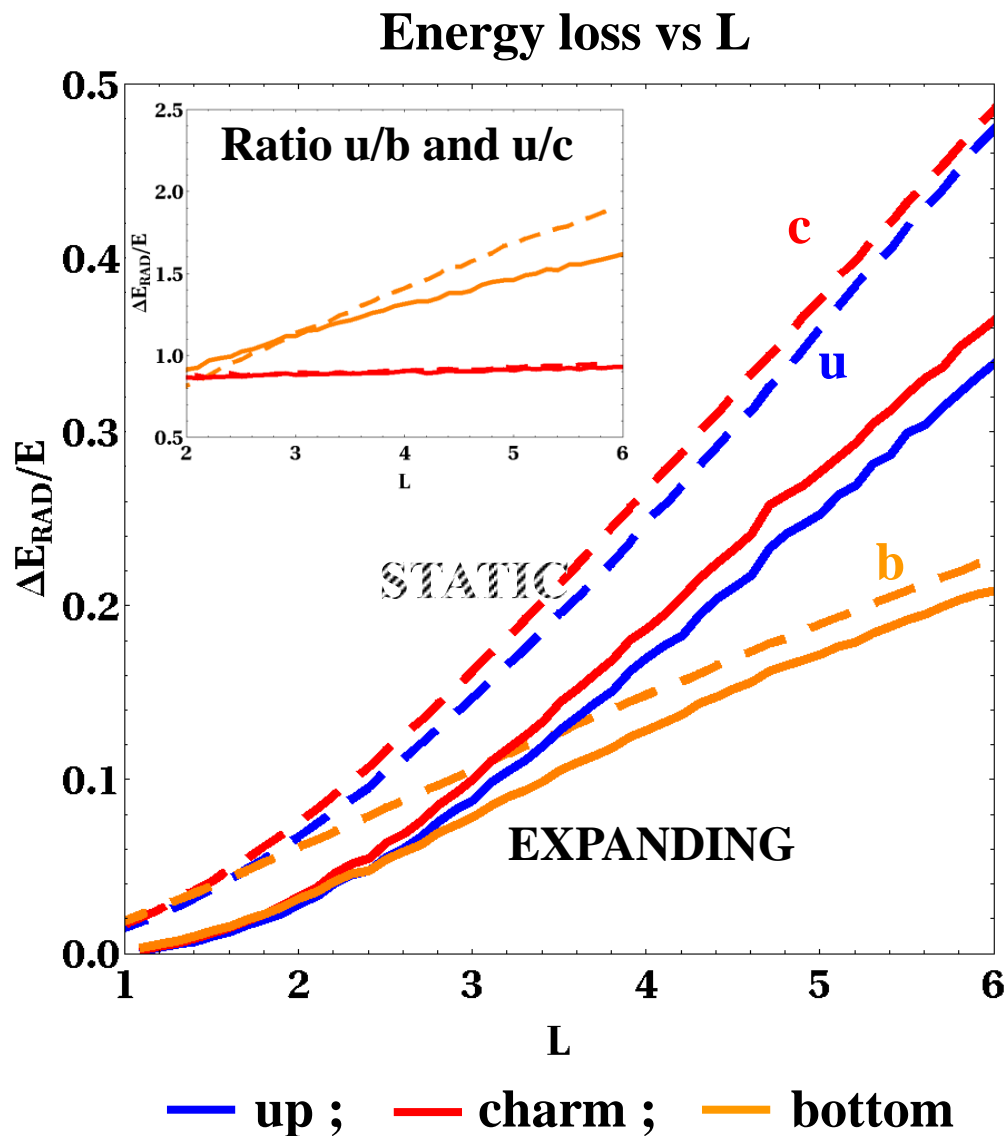


AdS/CFT

Jinfeng Liao, arXiv:1109.0271

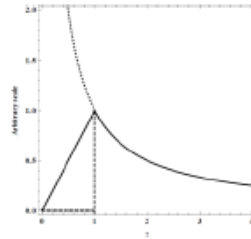


Energy loss

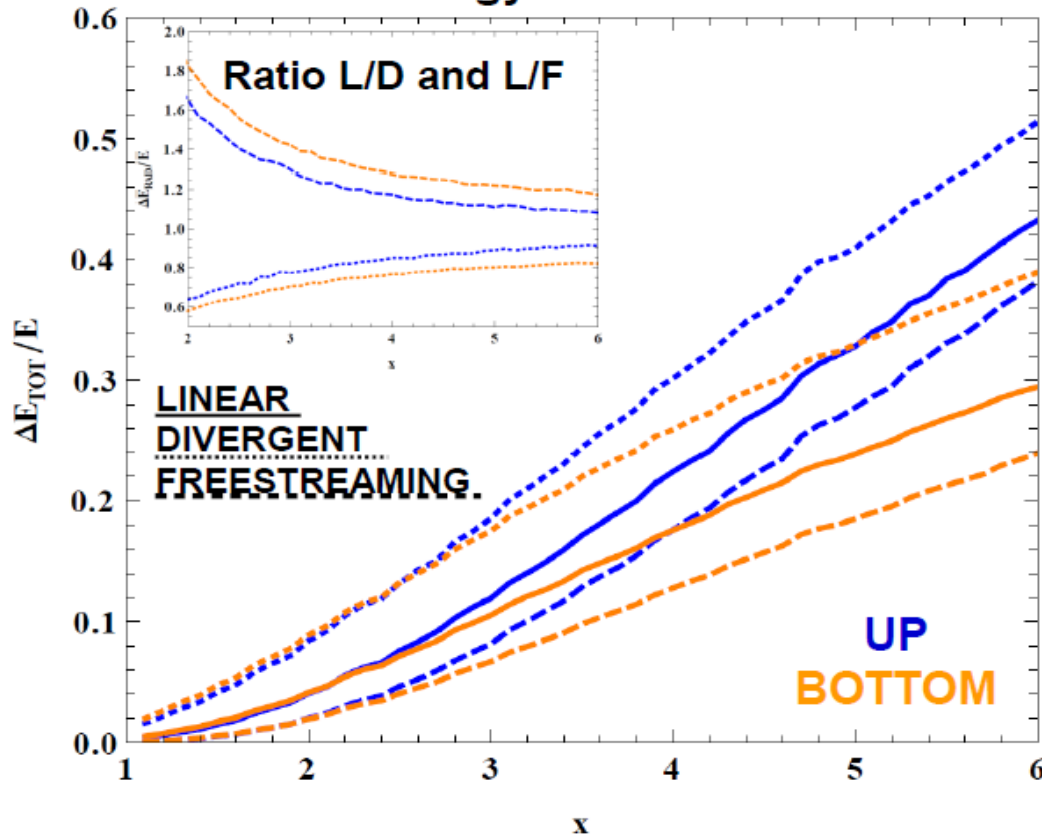


Temporal envelope

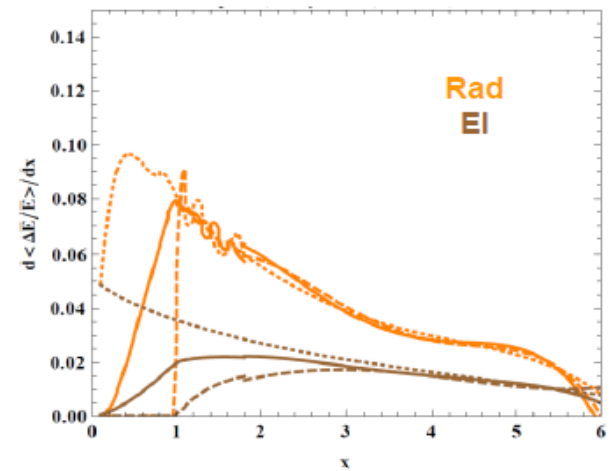
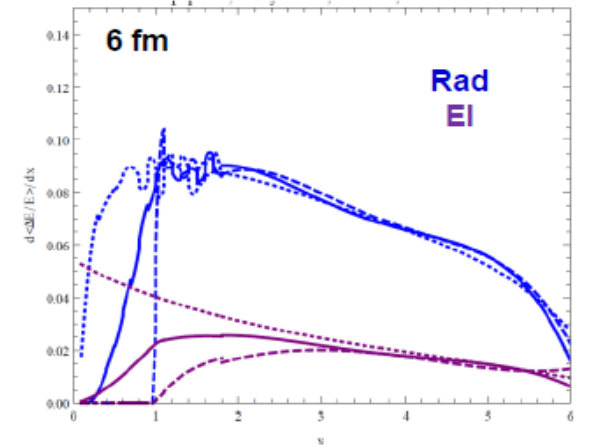
$$f\left(\frac{\tau}{\tau_0}\right) = \begin{cases} \frac{\tau}{\tau_0}, \frac{\tau_0}{\tau}, 0 & (\tau < \tau_0) \\ \frac{\tau_0}{\tau} & (\tau > \tau_0) \end{cases}$$



Energy loss vs L



Differential Energy Loss $\frac{d\langle\Delta E/E\rangle}{dx}$



k_T sensitivity

❖ Collinear approximation: $x_E = x_+ \left(1 + O\left(\frac{k_T}{x_+ E^+}\right)^2 \right)$

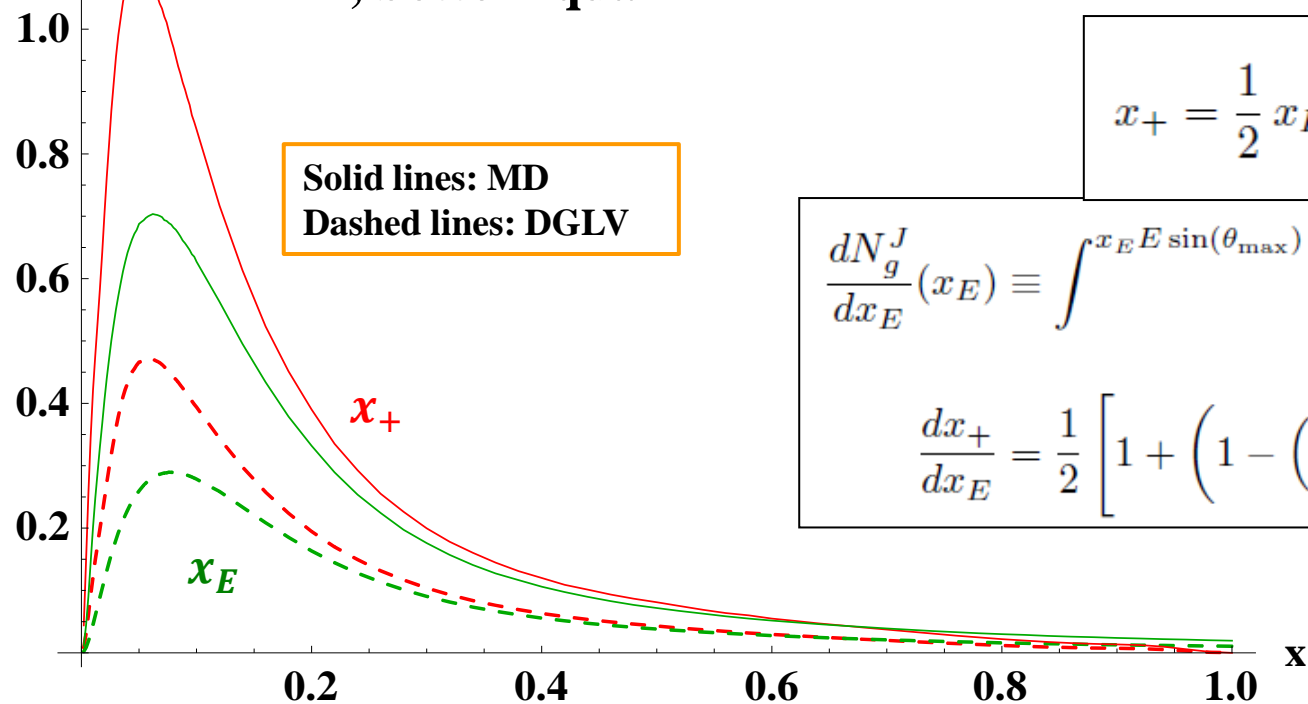
➤ DGLV formula has the same functional form for x_E or x_+

➤ Different kinematic limits: $k_T^{max} = x_E E$

$$k_T^{max} = 2E \text{Min}[x_+, 1 - x_+]$$

$x dN/dx$

L = 5, bottom quark



Solid lines: MD
Dashed lines: DGLV

x_+

x_E

$$x_+ = \frac{1}{2} x_E \left(1 + \sqrt{1 - \left(\frac{k_T}{x_E E}\right)^2} \right)$$

$$\frac{dN_g^J}{dx_E}(x_E) \equiv \int^{x_E E \sin(\theta_{max})} dk_T \frac{dx_+}{dx_E} \frac{dN_g}{dx_+ dk_T}(x_+(x_E)),$$

$$\frac{dx_+}{dx_E} = \frac{1}{2} \left[1 + \left(1 - \left(\frac{k_T}{x_E E}\right)^2 \right)^{-1} \right].$$

Poisson Ansatz (Buzzatti Thesis)

The simplest procedure for multiple gluon emission is the Poisson ansatz, where the number of emitted gluons follows a Poisson distribution, with the mean number \bar{N} given by the integral of the gluon emission spectrum $\bar{N} = \int dx \frac{dN_g}{dx}(x)$. After all, gluon radiation can be thought of as a stochastic event, and it makes sense to speak of a probability distribution $P(\epsilon)$ of radiating a certain amount of energy $\epsilon \equiv \Delta E/E$:

$$P(\epsilon) = P_0 \delta(\epsilon) + \tilde{P}(\epsilon)|_0^1 + P_1 \delta(1 - \epsilon) \quad (2.20)$$

The probability distribution is split in three components: the first term corresponds to the probability of zero radiation, $P_0 = e^{-\bar{N}}$. The second term is given by

$$\tilde{P}(\epsilon) = \sum_{n=1}^{\infty} P_n(\epsilon) \quad , \quad (2.21)$$

with

$$\begin{aligned} P_1(\epsilon) &= P_0 \frac{dN_g}{dx}(\epsilon \equiv x) \\ P_{n+1}(\epsilon) &= \frac{1}{n+1} \int_0^1 dx_n P_n(\epsilon - x_n) \frac{dN_g}{dx}(x_n) \end{aligned} \quad (2.22)$$

Dynamical potential divergence (Buzzatti Thesis)

The hybrid approach involves replacing the normalized static Debye screened momentum distributions in the DGLV multiple collision kernel

$$\prod_{i=1}^n dz_i d\mathbf{q}_i \sigma_{el}(\bar{v}^2(\mathbf{q}_i) - \delta^2(\mathbf{q}_i)) \rho(z_i) , \quad (4.4)$$

with an effective normalized magnetic enhanced transverse distribution

$$\bar{v}^2(\mathbf{q}; r_m) = \frac{\mathcal{N}(r_m)}{\pi} \frac{\mu_e^2}{(\mathbf{q}^2 + \mu_e^2)(\mathbf{q}^2 + r_m^2 \mu_e^2)} , \quad (4.5)$$

where $0 \leq r_m \equiv \mu_m/\mu_e \leq 1$ is the ratio of the color electric Debye and the assumed longer color magnetic screening lengths. The normalization factor

$$\mathcal{N}(r) = \frac{1 - r_m^2}{\log(1/r_m^2)} \quad (4.6)$$

reduces to unity when $r = 1$ but has a weak logarithmic zero for $r \rightarrow 0$. This zero is however canceled by the weak divergence of the effective elastic cross section $\sigma_{el}(r_m) = 9\pi\alpha_s^2/(2\mu_e^2\mathcal{N}(r_m))$. This no longer holds at opacity orders larger than one: the product of σ_{el} and $\delta^2(\mathbf{q})$ in Eq. (4.4), in fact, is still divergent. Fortunately, in the finite-size quark gluon plasma produced in A+A reactions, r_m is bounded from below by $1/(\mu_e R_A)$ due to confinement of color outside the plasma.

In the development of the hybrid model, we ignore the contribution arising from the mean free path $\lambda_{dyn} = c(n_f)^{-1}\lambda_{stat}$. The coefficient $c(n_f)$, which varies from $c(0) = 0.73$ to $c(\infty) = 1.09$, does not contribute much to the energy loss compared to the magnetically enhanced potential. Besides, its effect on $\Delta E/E$ can be easily reproduced with a small rescaling of the effective coupling.

Thermal Coupling

- ❖ In principle, the thermal coupling scale is given by the Debye mass itself, a self-consistent equation should be solved:

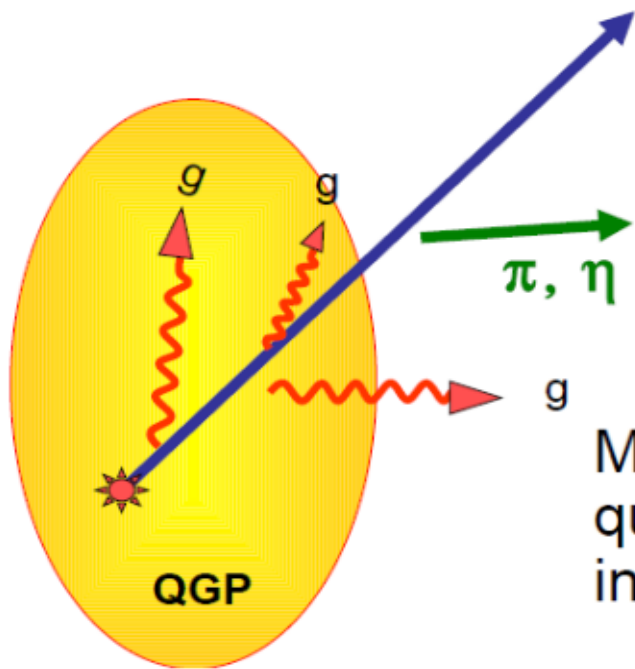
[Peshier, 2006]

$$m_D^2 = \frac{1}{3} N_c \left(1 + \frac{1}{6} n_f \right) 4\pi\alpha(m_D^2) T^2$$

Jet Tomography

Jet Tomography: GLV, DGLV, WHDG, CUJET1.0

Gyulassy, Levai, Vitev, Djordjevic, Wicks, Horowitz, Buzzatti



Quark or Glue Jet probes:

$$(\eta, p_T, \phi - \phi_{\text{reac}}, M_Q)_{\text{init}}$$

Hadron jet fragments:

$$(\eta, p_T, \phi - \phi_{\text{reac}})_{\text{final}}$$

Measurements of hadronic/leptonic quenching patterns provides information about QGP density

$$\Delta E^{\text{rad}} \propto \alpha_s^3 \int d\tau \tau \rho_{\text{QGP}}(\tau, \vec{r}(\tau)) \text{Log}\left(\frac{E_{\text{Jet}}}{T}\right)$$

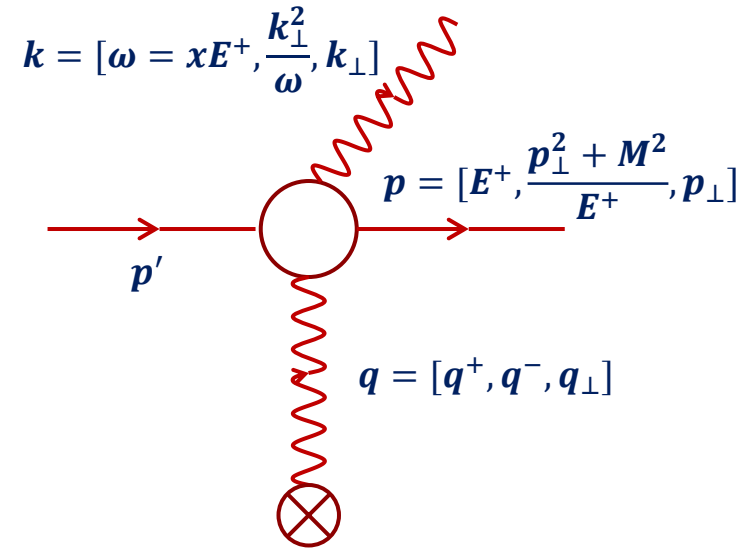
$$\Delta E^{\text{elas}} \propto \alpha_s^2 \int d\tau \rho_{\text{QGP}}^{2/3}(\tau, \vec{r}(\tau)) \text{Log}\left(\frac{E_{\text{Jet}}}{T}\right)$$

Radiative Energy Loss

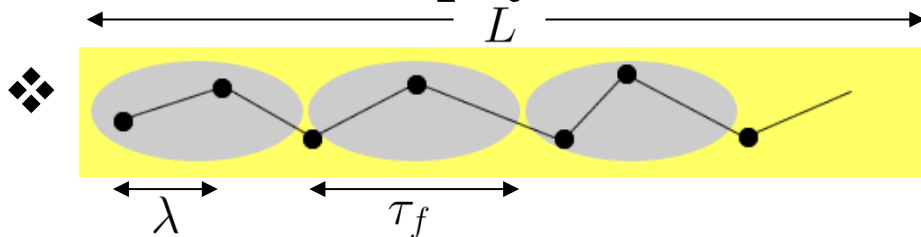
Incoherent limit: Gunion-Bertsch

$$\diamond \frac{dN}{dxdk_{\perp}} = \frac{1}{x} \frac{C_A \alpha_s}{\pi^2} \frac{q_{\perp}^2}{k_{\perp}^2 (q_{\perp} - k_{\perp})^2}$$

- Incoming quark is on-shell and massless
- The non-abelian nature of QCD alters the spectrum from the QED result
- Multiple scattering amplitudes are summed incoherently



Formation time physics



$$\tau_f \sim \frac{2\omega}{k_{\perp}^2}$$

- $\tau_f < \lambda < L$ Incoherent multiple collisions
- $\lambda < \tau_f < L$ LPM effect (radiation suppressed by multiple scatterings within one coherence length)
- $\lambda < L < \tau_f$ Factorization limit (acts as one single scatterer)